Design, Synthesis, and Biophysical and Biological Evaluation of a Series of Pyrrolobenzodiazepine−Poly(*N*-methylpyrrole) Conjugates

Geoff Wells,[†] Christopher R. H. Martin,[‡,§] Philip W. Howard,[†,‡] Zara A. Sands,[||] Charles A. Laughton,[||] Arnaud Tiberghien,[†,‡] Chi Kit Woo,[‡] Luke A. Masterson,[†,‡] Marissa J. Stephenson,[‡] John A. Hartley,[⊥,‡] Terence C. Jenkins,[#,▽] Steven D. Shnyder,[⊗] Paul M. Loadman,[⊗] Michael J. Waring,[§] and David E. Thurston*[,†,‡]

Cancer Research UK Gene Targeted Drug Design Research Group, The School of Pharmacy, University of London, 29/39 Brunswick Square, London WC1N 1AX, U.K., Spirogen Ltd, 2 Royal College Street, London NW1 0NH, U.K., Department of Pharmacology, University of Cambridge, Tennis Court Road, Cambridge CB2 1PD, UK, School of Pharmacy, University of Nottingham, University Park, Nottingham NG7 2RD, U.K., Cancer Research UK Drug-DNA Interactions Research Group, Department of Oncology, Royal Free and University College Medical School, UCL, 91 Riding House Street, London W1W 7BS, U.K., School of Pharmacy and Pharmaceutical Sciences, University of Manchester, Oxford Road, Manchester M13 9PL, U.K., and Cancer Research UK Cancer Research Unit, Institute of Cancer Therapeutics, University of Bradford, All Saints Road, Bradford, West Yorkshire BD7 3AY, U.K.

Received November 29, 2005

A novel series of methyl ester-terminated C8-linked pyrrolobenzodiazepine (PBD)−poly(*N*-methylpyrrole) conjugates (**50a**−**f**) has been synthesized and their DNA interaction evaluated by thermal denaturation, DNA footprinting, and in vitro transcription stop assays. The synergistic effect of attaching a PBD unit to a polypyrrole fragment is illustrated by the large increase in DNA binding affinity (up to 50-fold) compared to the individual PBD and pyrrole components. **50a**−**f** were found to bind mainly to identical DNA sequences but with apparent binding site widths increasing with molecular length and the majority of sites conforming to the consensus motif 5'-XGXW$_z$ ($z = 3 \pm 1$; W = A or T; X = any base but preferably a purine). They also provided robust sequence-selective blockade of transcription at sites corresponding approximately to their DNA footprints. **50a**−**f** were shown to have good cellular/nuclear penetration properties, and a degree of correlation between cytotoxicity and DNA-binding affinity was observed.

Introduction

Compounds that bind in the minor groove of DNA have found use in the experimental treatment of cancer and certain infectious diseases. Furthermore, agents which target and disrupt distinct DNA sequences have the potential to offer selective therapies by modulating the activity of specific transcription factors or genes. For this reason, a number of sequence-selective DNA-binding agents have been evaluated with a range of affinities and recognition fidelities. Of particular note are the hairpin polyamides[1] that combine high affinity DNA binding with good sequence discrimination, although variable nuclear penetration characteristics in cells have to date slowed their development as therapeutic agents.[2,3] The addition of a covalent binding motif to such molecules offers the possibility of targeting the coding regions of genes where the molecules may otherwise be dislodged by the advancing replication fork.[4] Such a covalent moiety may also have innate DNA sequence-recognition properties. In this respect, the pyrrolo[2,1-*c*][1,4]benzodiazepines (PBDs[a])[5] (e.g., **1**−**3** in Figure 1) are of interest as they bind to guanine residues in the minor groove with a preference for Pu-**G**-Pu sequences.

There has been significant recent research activity in the PBD area,[6−8] including previous reports of the synthesis and evaluation of conjugates containing a PBD moiety linked to various combinations of pyrroles and imidazoles. Lown has reported[9] the synthesis of PBD conjugates (termed PBD−lexitropsin conjugates) **9a**−**c** (Figure 2) with a four-carbon linker between the PBD C8-position and first heterocycle, and with a 3-(dimethylamino)propyl terminus. Although stated to be lexitropsin derivatives with the $n = 2$ and 3 analogues mimicking the linked *N*-methylpyrrole rings of **8** (netropsin) and **7** (distamycin), respectively, the 3-(dimethylamino)propyl tail differs from the amidinoalkyl tails of the natural products. Conjugates **9a**−**c** were

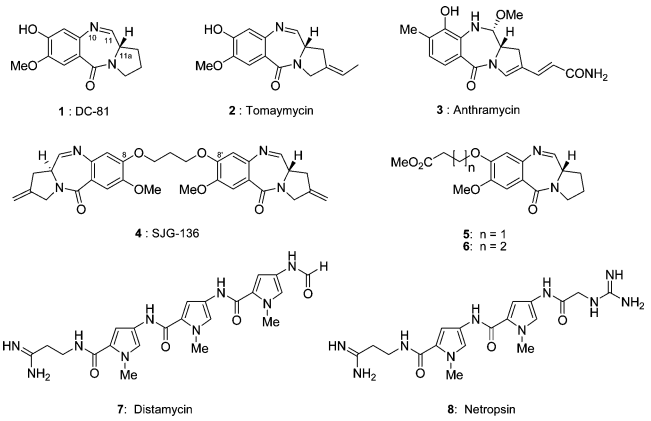

Figure 1. Structures of the PBD monomers (**1**, **2**, **3**, **5**, and **6**), the PBD dimer **4**, and distamycin and netropsin (**7** and **8**).

* Corresponding author. Phone: +44 0207 753 5931 (Direct) or +44 0207 753 5932 (Secretary) Fax: +44 0207-753-5935. E-Mail: david.thurston@pharmacy.ac.uk.
[†] University of London.
[‡] Spirogen Ltd.
[§] University of Cambridge.
[||] University of Nottingham.
[⊥] Royal Free and University College Medical School.
[#] University of Manchester.
[⊗] University of Bradford.
[▽] Present address: Morvus Technology Limited, Building 115, Porton Down Science Park, Salisbury, Wiltshire SP4 0JQ, U.K.

[a] Abbreviations: CT-DNA, calf thymus DNA; EMSA, electrophoretic mobility shift assay; ER, estrogen receptor; GI_{50}, concentration causing 50% growth inhibition; LC_{50}, concentration causing 50% cell kill; LTR, long terminal repeat; MD, molecular dynamics; PBD, pyrrolo[2,1-*c*][1,4]-benzodiazepine; TGI, concentration causing 100% growth inhibition; T_m, DNA helix to coil transition (melting) temperature; T-stop assay, transcription stop assay.

10.1021/jm051199z CCC: $33.50
Published on Web 08/05/2006

reportedly prepared in overall 28-30% yields as a mixture of their N10−C11 imine and carbinolamine methyl ether forms which were highly polar and soluble only in a $CHCl_3$−MeOH mixture but not sufficiently soluble in either solvent alone to allow separation of the pure forms. Compounds **9b** and **9c** had modest cytotoxicity in the NCI panel with average LC_{50} values ranging from 7.5 to 86.5 μM for **9b** ($n = 2$) to 0.9−93 μM for **9c** ($n = 3$).[10] Lown has also reported[11,12] the synthesis of three equivalent imidazole analogues (**10a**−**c**; $n = 1-3$) and two mixed pyrrole-imidazole analogues (**11a**,**b**; $n = 1-2$). These compounds, obtained in overall 35−40% yields, existed as 1:1 mixtures of imines and carbinolamine methyl ethers. Compounds **10a**−**c** ($n = 1-3$) were not significantly active in the NCI 60 cell-line panel, with mean GI_{50}, TGI, and LC_{50} values in the range of 16.2−95.5 μM, but conjugates **10b** and **10c** gave IC_{50} values of 14.4 and 4.4 μM, respectively, in K562 cells (48 h exposure). Similarly, **11a**,**b** showed no significant cytotoxicity with mean NCI GI_{50}, TGI, and LC_{50} values in the 20.9−95.5 μM range (5.2 μM in K562).

Baraldi and co-workers have reported[13] the synthesis of PBD-distamycin conjugates (**12c**, $n = 3$) and related analogues **12a**,**b** ($n = 1$ or 2) and **12d** ($n = 4$) which differ from the conjugates synthesized by Lown in having a three-carbon rather than a four-carbon linker, and in possessing the amidine terminus found in distamycin and netropsin rather than a 3-(dimethylamino)propyl residue. Although NCI data are not reported for these conjugates, **12c** is more cytotoxic ($IC_{50} = 0.2$ μM in K562 cells) than the Lown conjugates and slightly more potent than either the PBD fragment alone in the form of an ester (**5**, 1.0 μM) or distamycin A (>30 μM). Interestingly, **12d** was the most active conjugate reported with an IC_{50} of 0.04 μM in K562 cells (>100 μM and 6.0 μM for **12a** and **12b**, respectively). In the HL3T1 cell line (72 h incubation), **12a**−**d** had IC_{50} values of 50.0, 12.0, 2.5, and 1.0 μM, respectively. However, cytotoxicity evaluations in K562 cells (>100 μM [$n = 1$] to 0.04 μM [$n = 4$]) and Jurkat cells (80 μM [for $n = 1$] to 0.07 μM [for $n = 4$]) suggested that increasing the length of the polypyrrole backbone leads to enhanced in vitro activity. Only the $n = 3$ and $n = 4$ compounds were more potent than either the PBD fragment alone (**5**) or the relevant PBD-free polypyrrole.

Finally, in an effort to enhance water solubility, Lown and co-workers more recently reported[14] a set of sixteen PBD-heterocycle conjugates (**13a**−**h**) containing various numbers of pyrrole and imidazole units but with ring *N*-glycosylated heterocycles. In eight of these molecules the hydroxyl moieties of the glycosyl units were fully acetylated (R = Ac), and in the other eight all acetyl groups were absent (R = H). The acetylated and deacetylated analogues are directly comparable in structure to **9a**−**c** and **10a**−**c** but contain either one or two glycosyl units per molecule. Data from the NCI panel indicate that all molecules in the series **13a**−**h**, whether glycosylated or not, are significantly less cytotoxic than **9b**,**c** ($n = 2$ or 3). Also, although as a group, **13a**−**h** (R = H) are designed to be more water-soluble than their acetylated counterparts **13a**−**h** (R = Ac), the average IC_{50} values show only a marginal improvement due to just one compound **13h** (R = H). This conjugate shows a marked improvement compared to its acetylated equivalent (i.e., mean $LC_{50} = 0.59$ versus 93.3 μM for **13h** [R = H] and **13h** [R = Ac], respectively), although both compounds had IC_{50} values of >100 μM in K562 cells.

Limited DNA-binding data have been reported for the conjugates described above. For example, using a polymerase chain reaction (PCR) assay against the Ha-*ras* oncogene (G/C-rich) or estrogen receptor (ER) (A/T-rich) sequences, unlike distamycin A which inhibited PCR in only the A/T-rich sequence (or control PBD **5** which failed to inhibit PCR in either sequence), **12c** ($n = 3$) was equipotent in inhibiting PCR in both the G/C-rich and A/T-rich DNAs at a level of potency 6-fold higher than distamycin in the A/T-rich sequence. This demonstrated that the hybrid was much more active than either of its constituent parts in terms of DNA binding affinity. It also suggested that the sequence-selectivity of the hybrid was different from distamycin in binding to mixed rather than only A/T-rich sequences. For the extended set **12a**−**d**, Baraldi also investigated[15] sequence selectivity and stability of the DNA−drug complexes, and performed DNase I footprinting and arrested PCR assays on fragments of the human c-*myc* oncogene and human immunodeficiency virus type 1 long terminal repeat (HIV-1 LTR) (both G/C-rich), and the ER gene (A/T-rich) sequence. It was found that the ability of **12a**−**d** to arrest PCR of the c-*myc* ($IC_{50} = 2-6$ μM) and HIV ($IC_{50} = 0.8-2.0$ μM) gene targets was greater than for distamycin A (25 μM and 50 μM for c-*myc* and HIV, respectively), suggesting that the presence of the PBD might favor a shift towards G/C recognition. Interestingly, for the ER gene, **12a**,**b** were similar in activity ($IC_{50} = 3.0$ μM and 2.0 μM, respectively) to distamycin ($IC_{50} = 5\mu$M), whereas **12c**−**d** were marginally more active (0.8 μM and 0.2 μM, respectively) suggesting greater A/T-selectivity. Analysis of arrest sites for ER PCR suggested that **12a** arrests at 5′-AGTTTAAA-3′, whereas **12b**−**d** cause arrest at the same site but also at 5′-CATATATGTGTG-3′. Comparative footprinting experiments for **12a**−**d** suggested that changes in the number of pyrrole rings did not produce significant changes in sequence recognition; however, it was noted that the footprints generated by **12d** were larger than that generated by distamycin. Using a PCR-based dialysis experiment, it was demonstrated that hybrids **12a**−**d** exhibit different DNA-binding characteristics compared to either **7** (distamycin A) or the PBD (**5**). In addition, a direct relationship was found between the number of pyrrole rings present in the hybrids and the stability of the DNA−ligand complexes. Confirming the previous studies of Baraldi,[15] Gambari and co-workers reported[16] the effects of **12a**−**d** on the interaction of purified NF-κB and [^{32}P]-labeled oligomers that mimic the NF-κB HIV-1 LTR binding sites using both gel retardation (EMSA) and filter binding assays. The results showed that conjugates **12a**−**d** were effective in inhibiting NF-κB p52/ NF-κB DNA interactions by the EMSA assay although only **12b**−**d** were active according to the filter assay. Similarly, conjugates **12c**−**d** (but not **12a**) were shown to efficiently inhibit HIV-1 LTR-driven transcription in vitro whereas the PBD fragment **5** alone could not. Baraldi and co-workers[17] also reported that **12c** inhibits binding of the transcription factor Sp1, a protein important for the control of transcription of cellular and viral genes, to its cognate DNA sequence. Nuclear proteins were isolated from K562 cells and immobilized on a filter after electrophoresis. The ability of **12c** to inhibit the binding of [^{32}P]-labeled Sp1 oligomer to the filter was then studied. Although the PBD fragment (**5**) or distamycin A failed to inhibit binding at concentrations of up to 50 μM, conjugate **12c** completely blocked the Sp1/DNA binding interaction at 10 μM, a result which was confirmed by gel shift experiments. Gambari and co-workers also reported[18] IC_{50} values for **12a**−**d** in HL3T1 cells (72 h), confirming earlier observed trends of greater cytotoxicity with increasing numbers of attached pyrrole units. Interestingly, they also found that **12a**−**d** bind to TAR−RNA (particularly the structured TAR−RNA of HIV-1) and can inhibit TAR/protein interaction.

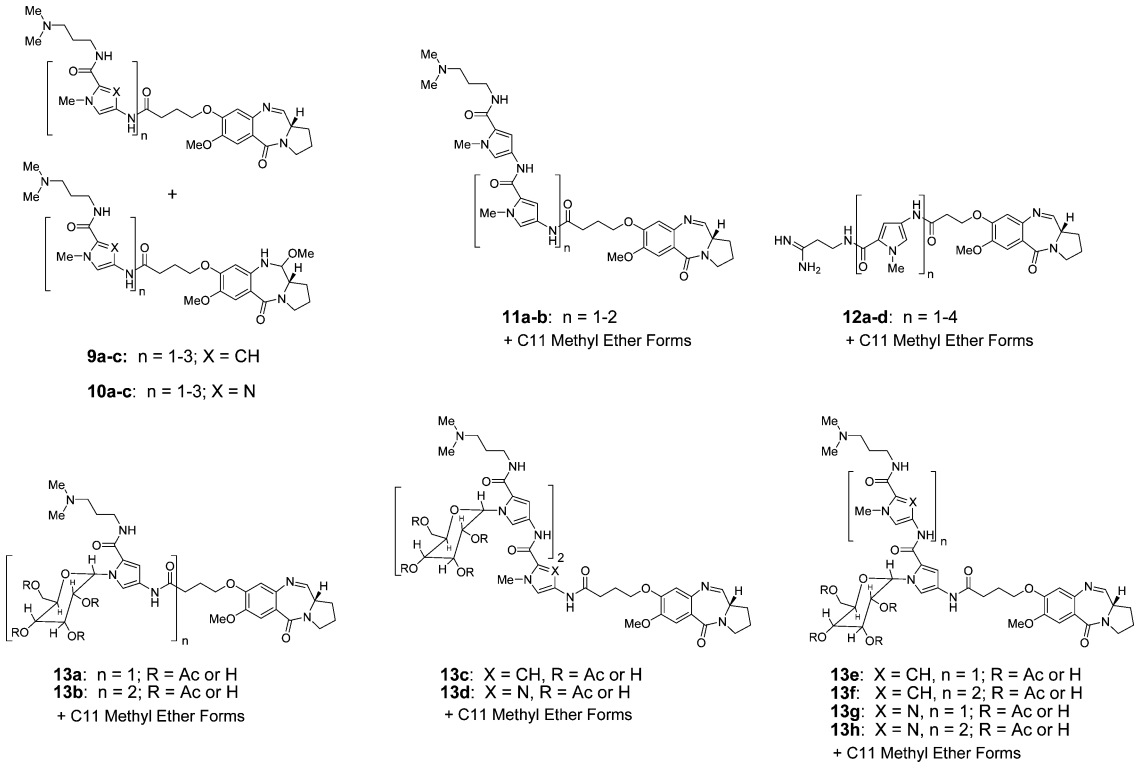

Figure 2. Structures of PBD−polypyrrole conjugates previously reported by Baraldi and Lown.

To further explore this class of molecules, we set out to extend the number of pyrroles attached to a PBD via the C8-position to six heterocyclic units and, as part of this process, to use molecular modeling to optimize the linkage between the PBD and polyheterocycle chain. Furthermore, we sought to explore a different tail (methyl ester) for the conjugates in contrast to the earlier reported 3-(dimethylamino)propyl or amidine termini. This has allowed us to show that the four-carbon link between the PBD and heterocycle tail is preferred as the conjugates are maintained in an isohelical structure more suitable for accommodation in the minor groove of DNA. We have used thermal denaturation, DNA footprinting, and in vitro transcription inhibition methodologies to evaluate both DNA-reactivity and sequence-selectivity and have also determined nuclear/cellular penetration and cytotoxicity in a number of human tumor cell lines. The results have revealed a surprisingly large synergistic effect upon joining the PBD and methyl ester-terminated polyheterocycle units through a four-carbon linker in terms of both the rate and extent of DNA binding and their in vitro cytotoxic potency.

Results and Discussion

Molecular Modeling. Before embarking on the synthesis program, initial molecular modeling studies were carried out to determine the optimum length for the linker joining the C8-position of the PBD to the amino group of the first heterocycle. The choices were a three-carbon link as used by Baraldi and co-workers (e.g. **12**, $n = 1-4$ in Figure 2) and as featured in **38**, or a four-carbon link as used by Lown and colleagues (e.g., **9**-**11** and **13a**−**h**) and as adopted for **50a**−**f**. Initial studies focused on the interaction of **38** within the DNA minor groove. Since covalent binding ("fixation") of the PBD unit to guanine is essentially irreversible at physiological pH, sequence-selective positioning of the ligand must occur prior to this event. Therefore, we sought to produce a model for the complex in which the imine functionality of the PBD was positioned appropriately for interaction, while other favorable and potentially sequence-reading interactions were made by the remainder of the molecule. However, extensive manual docking investigations made it clear that the limited flexibility of the three-carbon linker between the PBD and first heterocycle made it difficult to obtain a conformation of the conjugate that fully satisfied these requirements. In particular, conformations in which the three *N*-methylpyrrole rings fitted neatly and isohelically within the minor groove always resulted in the PBD unit rotating partially out of the groove, so that the six-membered A-ring of the PBD made poor contacts with the groove base. Conversely, if optimal interaction of the PBD moiety within the minor groove was enforced, the first *N*-methypyrrole ring 'bulged' out of the groove. One of the best manually docked conformations was subjected to a molecular dynamics (MD)-based relaxation and conformational sampling process in order to see if this could be improved. For this we used a Generalized Born (GB) solvation model and restrained the DNA close to a canonical B-form helix so that the 'fitness' of the ligand for the DNA was the key factor, rather than any plasticity in the DNA itself. Use of the GB model allowed a reasonable sampling of conformational space by the ligand within a limited simulation time frame, due to the absence of solvent damping effects. The PBD portion of the ligand remained suitably poised for interaction between the imine center and the guanine N2, but the overall orientation of **38** in the minor groove was still poor (Figure 3A).

This led us to investigate the effect of adding an additional methylene unit to the linker between the PBD and the polypyrrole sections of the ligand (i.e., **50c**). Manual docking of **50c** into the DNA minor groove was performed as before, and it was immediately evident that a much more isohelical ligand conformation was readily achievable. The docked conformation was subjected to the same MD analysis as before. Again, through dynamics the ligand explored a reasonable region of conformational space, but remained suitably placed for the

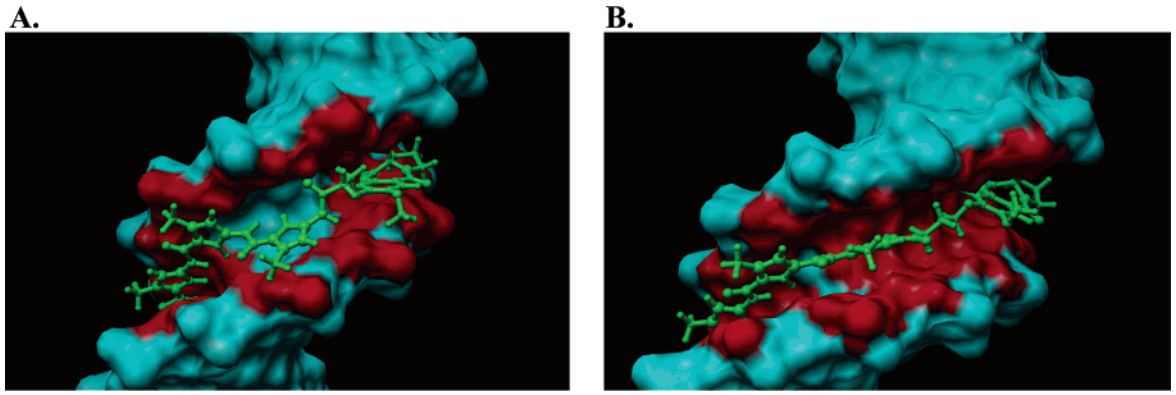

Figure 3. Time-averaged structures of **38** (A) and **50c** (B) bound to the 17-mer DNA duplex 5′-TTTTGCAAAAAGCTTCA-3′ (guanine adjacent to the PBD C11-position is underlined). In each case, sections of the molecular surface of the DNA less than 5 Å from the ligand are colored red to emphasize the superior fit of **50c** (B) in the minor groove compared to **38** (A).

Scheme 1[a]

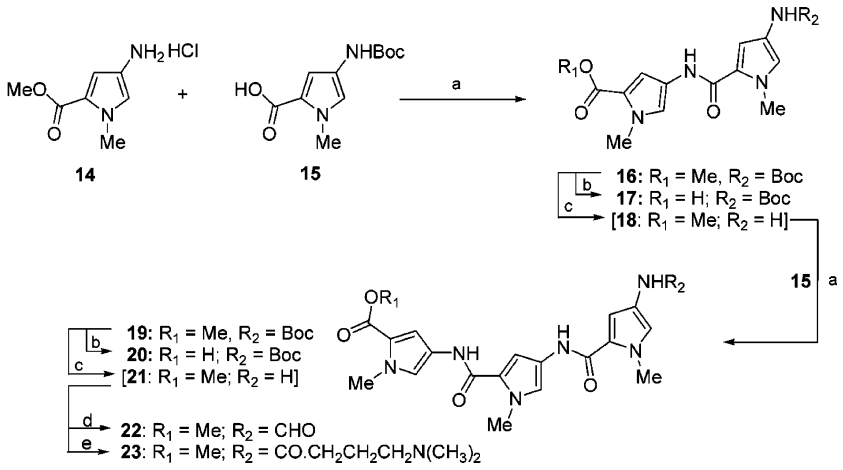

[a] (a) EDCI, DMAP, CH_2Cl_2, 18 h, 48−94%; (b) NaOH, H_2O, MeOH, 74−100%; (c) 4M HCl in dioxane, 30 min; (d) EDCI, DMAP, HCO_2H, CH_2Cl_2, 18 h, 60%; (e) EDCI, DMAP, 4-(dimethylamino)butyric acid, CH_2Cl_2, 96 h, 81%. Compounds **18** and **21** were formed in situ and used directly in the next steps.[22−24]

alkylation reaction and with a highly isohelical geometry (Figure 3B). The apparent superiority of **50c** was confirmed by the calculation of relative binding affinities, using the MM-GBSA method.[19] Binding energies were estimated to be -14 ± 3 kcal mol^{-1} and -26 ± 6 kcal mol^{-1} for **38** and **50c**, respectively.

This method does not represent a 'state-of-the-art' attempt to predict the structural and energetic features of the ligand-DNA recognition process, as the simulations were short, the DNA was restrained, and an approximate solvation model was used. Nevertheless, these calculations do provide a good qualitative indication that a four-carbon linker should be superior in terms of binding behavior. On this basis, the synthesis of the **50a**−**f** series was planned in conjunction with the appropriate controls **6**, **22**, **23**, and **56** for comparison.

Synthesis. The pyrrole amino ester (**14**) and Boc-protected pyrrole amino acid (**15**) prepared as described previously[20] were coupled using a solution-phase method (EDCI and DMAP) so that the reaction could be easily monitored, with workup involving simple solvent extraction to furnish the product in sufficient yield and purity to use in subsequent steps[21] (Scheme 1). The resulting *N*-Boc dipyrrole (**16**) was deprotected to give **18**[22−24] which was followed by a second coupling reaction with **15** to give the Boc-protected trimer pyrrole (**19**). Saponification or Boc-deprotection of esters **16** and **19** provided the corresponding dimer and trimer acids (**17** and **20**) or the amino esters (**18** or **21**), respectively, that were used to make the higher homologues in the series. Reaction of the amino (**18**) and acid

Scheme 2[a]

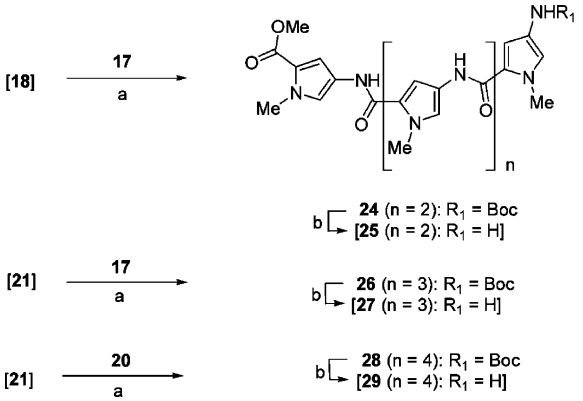

[a] (a) EDCI, DMAP, CH_2Cl_2, 48 h, 54−90%; (b) 4M HCl in dioxane, 30 min. Compounds **25**, **27**, and **29** were formed in situ and used directly in the next steps.[22−24]

(**17**) dimers afforded the tetrapyrrole fragment **24** which could be Boc-deprotected to give **25**[22−24] (Scheme 2). Similarly, the Boc-deprotected trimer **21**[22−24] could be reacted with either the acid dimer (**17**) or trimer (**20**) to give the Boc-protected pentapyrrole (**26**) or hexapyrrole (**28**) molecules. These could be Boc-deprotected to give **27** or **29**,[22−24] respectively. It should be noted that **18**, **21**, **25**, **27**, and **29** were prepared in situ and used directly in the next steps. The control molecules **23** and

Scheme 3[a]

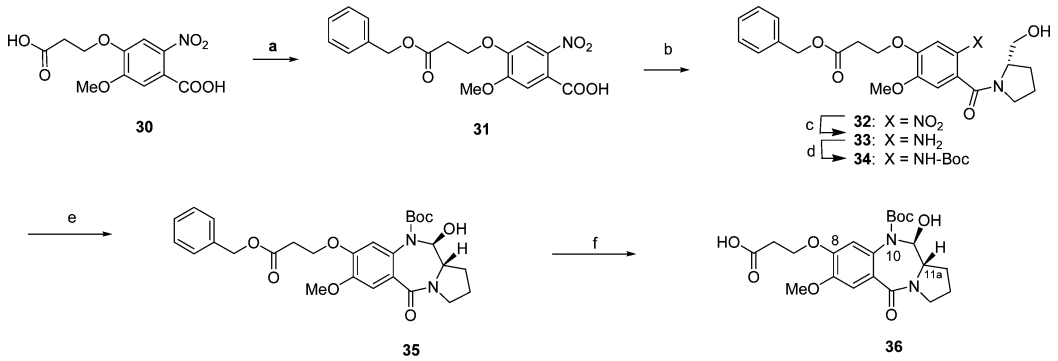

[a] (a) $PhCH_2OH$, cat. 4-TsOH, toluene, 3.5 h, 56%; (b) (i) $(COCl)_2$, DMF, CH_2Cl_2, 18 h; (ii) (2*S*)-(+)-pyrrolidinemethanol, Et_3N, −30 °C to RT, then overnight, 100%; (c) $SnCl_2 \cdot 2H_2O$, MeOH, reflux, 6 h; (d) $(Boc)_2O$, THF, reflux, 18 h; (e) pyridinium dichromate, CH_2Cl_2, 4 Å sieves, 4 h, 27% (three steps); (f) 10% Pd/C, H_2 (16 psi), EtOH, 100%.

Scheme 4[a]

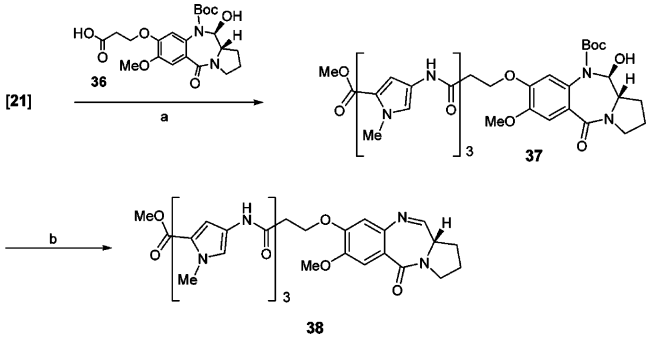

[a] (a) EDCI, DMAP, CH_2Cl_2, 18 h, 65%; (b) 95% aq. TFA, −10°C, 3 h, 96%.

22, chosen to represent the pyrrole portions of the conjugates with and without a four-carbon linker, were prepared by reacting the tripyrrole amine (**21**) with either formic acid or 4-(dimethylamino)butyric acid, respectively[21] (Scheme 1).

The Boc-PBD C8-propanoic acid (**36**) was synthesized using a modified Fukuyama approach (Scheme 3).[25] The side-chain carboxylic acid of **30**[26] was selectively esterified with $PhCH_2$-OH under acidic conditions to give **31**, and this was coupled to (*S*)-pyrrolidine methanol at −30 °C to furnish the nitro alcohol **32**. Reduction of the nitro group was followed by Boc protection of the resulting amine (**33**) to give **34**. Treatment of the primary alcohol with pyridinium dichromate effected oxidation and spontaneous ring closure to provide the N10-Boc-protected PBD **35** in 27% yield over three steps. Removal of the benzyl group from the C8 side-chain by catalytic hydrogenation gave the C8-propanoic acid PBD (**36**)[27] in quantitative yield. The PBD-tripyrrole conjugate with the three-carbon linker (**38**) was prepared by coupling the tripyrrole amino ester fragment (**21**), prepared in situ from **19**, to the PBD capping unit (**36**) (Scheme 4). The resulting conjugate intermediate (**37**) was Boc-deprotected to give the imine-containing PBD conjugate **38**.

The set of conjugates **50a**−**f** with each containing the four-carbon linker required the synthesis of a different PBD capping unit (**48**) as shown in Scheme 5. Vanillin (**39**) was initially coupled to methyl 4-bromobutyrate to give the ester aldehyde **40**.[28] Subsequent nitration (**41**[28]), oxidation (**42**), and coupling to (*S*)-pyrrolidine methanol gave the key nitro alcohol **43**, which was subsequently reduced (**44**) and N-Alloc-protected (**45**). Oxidative cyclization under Swern conditions gave the cyclized N10-Alloc-protected PBD ring system (**46**[29]). At this stage, hydrolysis of the methyl ester was required to provide the free acid capping unit. However, saponification with aqueous NaOH in MeOH led to racemization at the C11a position, a phenomenon first noted by Tercel and co-workers.[29] This is thought to arise from ring opening, enolization, and subsequent ring closure under the basic conditions of the reaction which results in loss of stereochemistry at C11a. To prevent this, and also to overcome the problem of competing ester formation during coupling reactions, a number of protecting group strategies were investigated for the C11-OH group. While protection with silicon-based protecting groups (i.e. TBDMS or TIPS) or acetate could be achieved, these groups were not stable to ester saponification and also led to racemization. Methylation at C11-OH could be achieved using MeI and Ag_2O; however, the AgOH byproduct induced partial (i.e., ∼10%) loss of C11a-stereochemistry as observed by chiral HPLC. Also, the methyl group was resistant to the ester hydrolysis step, and no further racemization was seen during this process. However, the most effective protecting group regarding the preservation of C11a stereochemistry was found to be THP, which was introduced easily using DHP and a catalytic amount of 4-toluenesulfonic acid to give **47** in quantitative yield. Although this product was a mixture of diastereomers due to the mixed stereochemistry at the pyran C2-position of the THP protecting group, ester hydrolysis gave the desired acid (**48**) in chirally pure form at C11a. This was confirmed by re-esterification followed by THP removal to give material that was equivalent by chiral HPLC to compound **46**. Treatment of the methyl ester **47** with Pd-$(Ph_3P)_4$ and pyrrolidine removed the Alloc and C11-*O*-THP protecting groups to afford the PBD **6** in 98% yield.

The C11-*O*-THP PBD acid capping unit **48** was coupled to the six individual amino acid pyrrole oligomers **14**, **18**, **21**, **25**, **27**, and **29** to generate conjugates **49a**−**f** (Scheme 6). Treatment with $Pd(Ph_3P)_4$ and pyrrolidine resulted in concerted removal of the N10-Alloc and C11-*O*-THP protecting groups to give the pure target PBD imine conjugates **50a**−**f** in 50−95% yield after purification by chromatography.

The non-imine-containing PBD-tripyrrole dilactam conjugate **56** was synthesized by a similar route (Scheme 7). The benzylated nitro vanillic acid **51** was coupled to L-proline methyl ester to give **52**, which cyclized to dilactam **53** in 88% yield after hydrogenation over 10% Pd/C in EtOH. The C8-butanoic acid linker was installed by reaction with benzyl 4-bromobutyrate/K_2CO_3 to give **54**, which was subsequently debenzylated by hydrogenation to give the free acid (**55**). Reaction of this with the amino ester tripyrrole fragment **21** afforded the tripyrrole PBD dilactam **56**.

Thermal Denaturation Studies. The relative reactivity and affinity of the hybrid molecules toward double-stranded DNA

Scheme 5[a]

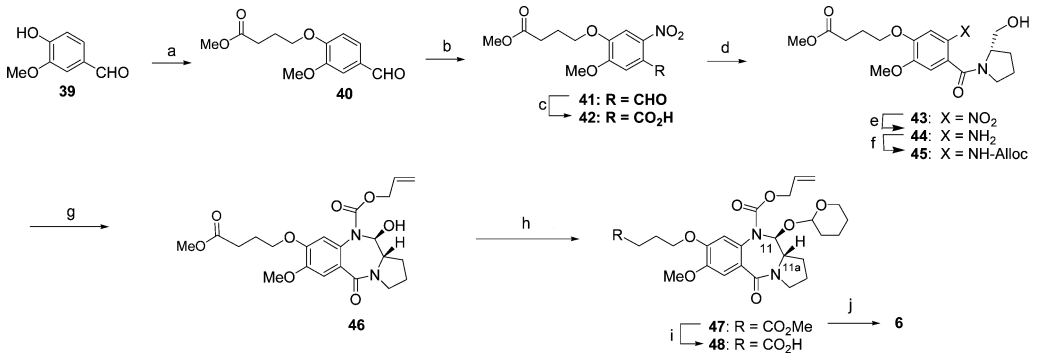

[a] (a) $Br(CH_2)_3CO_2CH_3$, K_2CO_3, DMF, 16 h, 85%; (b) 70% HNO_3, Ac_2O, 2.5 h; (c) $KMnO_4$, acetone, H_2O, 1 h, 50% (two steps); (d) (i) $(COCl)_2$, DMF, CH_2Cl_2, 18 h; (ii) (2*S*)-(+)-pyrrolidinemethanol, Et_3N, −30 °C to RT, then overnight, 100%; (e) 10% Pd/C, H_2 (45 psi), EtOH; (f) Alloc-Cl, CH_2Cl_2, 18 h, used without further purification; (g) DMSO, $(COCl)_2$, Et_3N, −40 °C, 62% (three steps); (h) DHP, cat. 4-TsOH, EtOH, 2 h, 100%; (i) NaOH, H_2O, 15 min, 98%; (j) $Pd(PPh_3)_4$, pyrrolidine, CH_2Cl_2, 1 h, 98%.

Scheme 6[a]

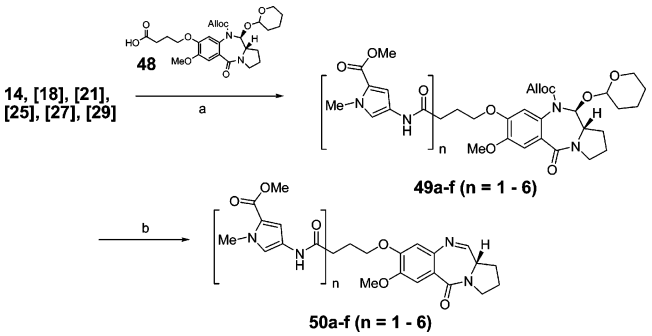

[a] (a) EDCI, DMAP, CH_2Cl_2, 24 h, 23−88%; (b) $Pd[PPh_3]_4$, pyrrolidine, CH_2Cl_2, 2 h, 50−95%.

was assessed from their induced effects upon the melting behavior (T_m) of calf thymus DNA. The thermal denaturation data shown in Table 1 provide unequivocal evidence that the PBD and polyheterocycle fragments contribute to overall effect in a synergistic manner. First, it is important to note the greater ΔT_m shifts for **50c** compared to **38**, thus confirming our modeling predictions for superiority with the four- rather than the three-carbon linker. The ΔT_m values for **50c** are >2-fold greater than those for **38** (following 0, 4, or 18 h incubation at 37 °C), indicating that the longer homologue has a greater stabilizing effect on the DNA duplex. Furthermore, the increased ΔT_m shifts seen for **50a**−**f** and **38** upon longer incubation are consistent with a time-dependent covalent mode of DNA interaction (i.e. "fixation" or bonding), following the faster initial component of reversible binding. This behavior is expected for any molecule containing a PBD unit.[26,30−38]

The ΔT_m values for the series **50a**−**f** reveal an increase in binding-induced DNA stabilization upon lengthening from one to three pyrrole units (i.e., **50a** → **50c**), followed by a subsequent decline to lower but still highly significant values as the side-chain is further extended. Interestingly, the control molecule **6**, which is a PBD with a similarly saturated and unsubstituted C-ring and a four-carbon linker but without pyrrole units, gives modest ΔT_m values of only 0.2, 0.3, and 0.4 °C (after 0, 4, and 18 h). The progressive kinetic increase in ΔT_m upon incubation indicates that this molecule interacts covalently with DNA, although conferring a much reduced level of overall stabilization. As expected, the ΔT_m shifts induced by **6** are similar to those obtained for the naturally occurring PBD monomer **1** (DC-81, Figure 1). The slightly higher effect may reflect an enhanced stability for the DNA adduct due to accommodation of the ester-terminated C8-linker in the host minor groove. However, the markedly increased ΔT_m values observed upon attaching between one to six pyrrole units (i.e., **50a** → **50f**) suggests that these heterocycles are also interacting in the minor groove and further enhancing DNA stabilization. Also the progressive increases in ΔT_m for each conjugate upon incubation clearly demonstrates that the pyrrole units do not interfere with the covalent DNA-binding ability of the PBD unit.

The second type of control molecules were the tripyrrole analogues **23** and **22**, comprising the tripyrrole unit of **38** and **50c** but with either 4-(dimethylamino)butyryl or formyl residues added to the *N*-terminus. These compounds, designed to gauge the DNA-binding efficiency of the polypyrrole fragment alone with or without a linker, increased the melting temperature of DNA by 5.5 and 4.3 °C, respectively (with no incubation). No significant increases in ΔT_m were seen after incubation as would be expected for a reversible, noncovalent mode of binding. The third type of control molecule, **56**, is a modified version of **50c** (i.e., a PBD conjugate with three pyrrole units) where the N10−C11 imine moiety is replaced with an inert amide (i.e., a PBD dilactam[39]) that cannot interact with DNA in a covalent manner. The time-independent behavior of ΔT_m for this dilactam upon incubation indicates that it binds reversibly without a slow secondary covalent component to its binding profile, as would be expected for an inactivated PBD. We have previously reported analogous behavior (i.e., $\Delta T_m = 2.9-3.3$ °C) for simple PBD dilactams that contain C-ring functionalization.[39] The ligand-induced ΔT_m shift for **56** is significantly smaller than that seen for the tripyrrole control molecules **22** and **23**, suggesting that the "neutralized" PBD unit presented by the dilactam may actually hinder accommodation of the oligopyrrole tail in the minor groove.

Table 1 illustrates the pronounced synergistic effect on ΔT_m of linking pyrrole units to the PBD moiety through the C8-position of the A-ring. For example, subunits **6**, **22**, and **23** give ΔT_m values (after 0−18 h incubation) of 0.2−0.4, 4.2−4.3, and 5.5−5.6 °C, respectively, whereas induced ΔT_m shifts of 17.3, 19.6, and 21.2 °C (at 0, 4, and 18 h) are obtained when two of these components are combined to give **50c**. This remarkable synergy was unexpected and is most likely due to either (i) an increased length of spanned DNA and enhanced covalent binding affinity, or (ii) the formation of "bis" adducts consisting of two molecules binding in antiparallel mode at the site. To put the ligand-induced ΔT_m shifts for the highest-affinity compound **50c** in context, the PBD dimer **4** (SJG-136, Figure 1), a sequence-selective covalent interstrand DNA cross-linking agent, was recently reported[33] to induce the greatest known effect upon T_m to date. Interestingly, **50c** stabilizes DNA toward

Scheme 7[a]

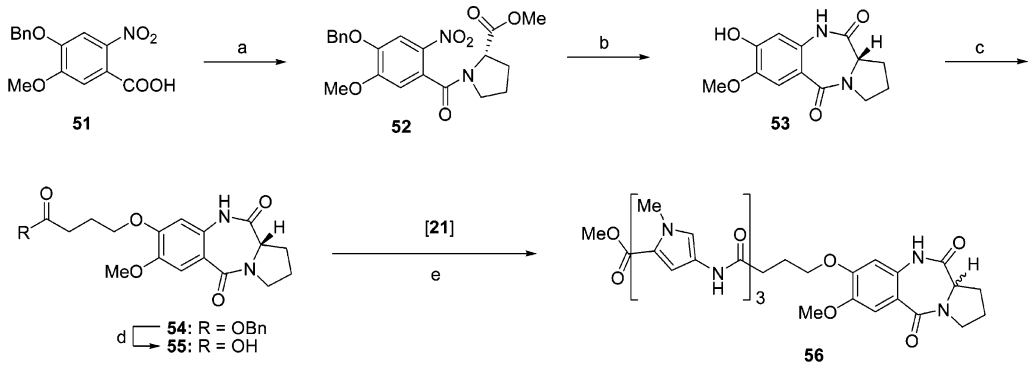

[a] (a) (i) $(COCl)_2$, DMF, CH_2Cl_2; (ii) L-proline methyl ester hydrochloride, Et_3N, CH_2Cl_2, −30 °C, 97% (over two steps); (b) 10% Pd/C, H_2, EtOH, 88%; (c) K_2CO_3, 4-bromobutanoic acid benzyl ester, DMF, overnight, 62%; (d) 10% Pd/C, H_2, EtOH, 100%; (e) EDCI, DMAP, CH_2Cl_2, 24 h, 6% (as a racemic mixture after preparative HPLC).

thermal denaturation even more effectively than **4** but without any requirement to form covalent interstrand DNA cross-links.

DNA Footprinting. The sequence selectivity of the six PBD−pyrrole conjugates (**50a**−**f**) and the control molecules (**6**, **22**, **23** and **56**) was evaluated by standard DNase I footprinting methods using the MS2 fragment which was designed by Fox and co-workers to contain every possible combination of tetranucleotides.[40] Conjugates **50a**−**f** were found to bind to the MS2 fragment at several locations. However, despite differences in binding affinity between each compound in the set, the footprinting patterns were surprisingly similar. A DNase I footprinting gel for **50c**, the conjugate effecting the largest ΔT_m shifts, on the MS2F (forward labeled) DNA fragment is shown in Figure 4. Footprinting gels for the other conjugates **50a**,**b** and **50d**−**f** for the MS2F fragment are shown in Supporting Information (S1, A−D). An example of a footprint on a MS2R (reversed labeled) fragment is shown (for **50e**) in S1-C.

The vast majority of footprint sites are common features in the binding profiles of all six conjugates, with only a small number of sites being footprinted by a subset of the family. Even more unexpectedly, no site is footprinted by only one molecule (in fact, the fewest number of conjugates that bind at any single site is four). The differential cleavage plot (Figure 5) provides footprinting profiles (color-coded for each conjugate) which illustrate a striking degree of overlap. Although there is no conspicuous change in footprinting patterns as the number of pyrrole units in each conjugate increases, there are changes in two other features, namely, the apparent binding affinity and the width of the footprinted site. The binding affinity of each molecule at a particular site was estimated (using the individual DNase I footprint images) as the concentration of conjugate providing 50% inhibition of DNase I-mediated cleavage at that site (i.e., DNase IC_{50}). To simplify comparison between molecules, one significant footprint site (5'-^{62}CAATACACA^{70}-3'/3′-GTTATGTGT-5′) was selected for comparison (Band "C" in Figures **4** and **5**). Using this approach, **50d** (four pyrroles) appears to be the strongest binder with a DNase IC_{50} of around 30 nM. Conjugates **50c** (three pyrroles) and **50e** (five pyrroles) follow closely with affinities in the region of 30−100 nM. Conjugates **50b** (2 pyrroles) and **50f** (6 pyrroles) are poorer binders but still exhibit nanomolar affinities in the region of 100−300 nM and 300 nM, respectively. Finally, **50a** (one pyrrole) is a weak footprinting molecule with a DNase IC_{50} value of approximately 10 μM. In terms of a possible relationship between binding site width and length of the PBD conjugates, inspection of sites B and C in Figure 5 suggests that, compared to the shortest conjugate **50a** (red line), the longer conjugates appear to have larger binding site widths, although there is not a perfect correlation.

The binding characteristics of the **50a**−**f** series at all thirteen sites within the MS2 DNA fragment are provided in detail in Figures S2A and S2B (Supporting Information). The same site ("C"; 5'-^{62}CAATACACA^{70}-3') and its close neighbor 5'-^{50}-ATCCATATGCG^{60}-3' ("B") were also chosen and analyzed in order to assess the effect of increasing the size of the molecules on the length of the bound sequence. It appears that, as additional pyrroles are added to the PBD, there is a consequent rise in the number of base pairs within the associated binding site. This positive correlation is suggestive of larger tracts of DNA becoming bound by molecules of increasing length, although it is not yet known whether the effect observed at any given site results from the binding of single molecules or more.

To assess the relative contributions of both the PBD subunit and the polypyrrole fragment in the **50a**−**f** series, the two control molecules **6** and **23** were examined and compared to **50c** (Figure 4). Interestingly, **6** does not produce any inhibition of DNase I-mediated cleavage at concentrations of up to 100 μM (cf. **50c** binding at 30−100 nM). In contrast, polypyrrole **23** produces a vivid footprinting pattern that shows significant overlap with that of **50c** apart from a few deviations (Figure 4, and detailed analysis of binding sites in S3, Supporting Information). These differences include the areas around positions 70−75 (5'-ATGGCC-3'), 90−95 (5'-CTAGTC-3'), 178−185 (5'-GGTCT-GTT-3'), and 197−202 (5'-GCCTCG-3'). One site (5'-^{185}-TTTGTC^{190}-3') is bound strongly by **23** alone. It is also interesting to note that the DNase IC_{50} value of **23** is 100-fold higher (~10 μM) than that of **50c** (~100 nM) at sites to which both molecules bind, presumably reflecting the covalent interaction of the PBD unit.

Given the failure of **6** to yield a useful footprint, anthramycin itself (**3** in Figure 1) was evaluated under similar conditions (S4, Supporting Information). This molecule produced several impressive footprints as previously documented in the literature,[5] although few coincided with those of **50a**−**f** (or **23**). Nearly all of the footprints produced by anthramycin correspond to the well-established 5′-PuGPu-3′ binding motif.[5] The most probable footprint sites included 5′-^{51}TCC^{53}-3′ (denoted *B*′; 5′-^{53}GGA^{51}-3′ on the complementary labeled strand), 5′-^{123}TCT^{125}-3′ and 5′-^{128}CCT^{130}-3′ (*K*′ and *L*′; 5′-^{125}AGA^{123}-3′ and 5′-^{130}AGG^{128}-3′ on the lower strand) and 5′-^{214}TCT^{216}-3′ which is 5′-^{216}-AGA^{214}-3′ (*U*′) on the lower strand. Some footprints are visible at less favored 5'-PyGPu-3′ sequences, e.g., 5′-^{71}TGG^{73}-3′ (*C*′) and 5′-^{86}TGC^{88}-3′ (*E*′). For the full list of 23 footprints see S4

Table 1. Cytotoxicity and Thermal Denaturation Data for the PBD−Pyrrole Conjugates **38** and **50a**−**f**, the Control Molecules **6**, **22**, **23**, and **56**, and the PDB Monomer **1** and Dimer **4**

Compound	Structure	NCI Screen (μM)			K562 96 h (μM)	Induced ΔT_m (°C)[ab] after incubation		
		GI_{50}	TGI	LC_{50}	GI_{50}	0 h	4 h	18 h
38	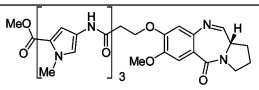	0.047	1.76	56.2	0.346	7.9	8.4	9.6
50a	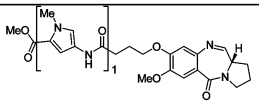	0.047	0.323	11.5	0.051	6.5	7.9	8.1
50b	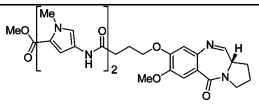	0.011	0.12	10.0	0.0071	13.9	15.0	15.6
50c	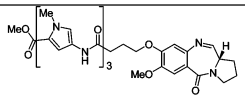	0.015	0.032	1.07	0.041	17.3	19.6	21.2[c]
50d	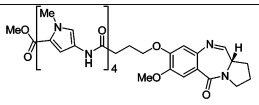	0.007	0.018	1.51	0.047	16.0	18.5	19.0[d]
50e	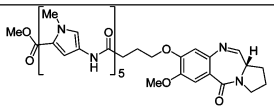	0.009	0.029	1.26	0.083	15.1	15.9	17.1
50f	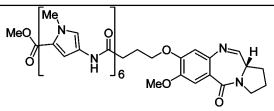	0.008	0.054	1.90	0.030	12.6	13.7	14.1
22	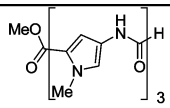	16.6	44.7	85.1	>10	4.3	4.2	4.2
23	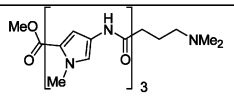	72.4	>100	>100	>10	5.5	5.5	5.6
56	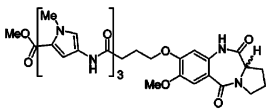	49.0	>50	>50	>10	1.1	1.1	1.2
6	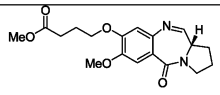	1.74	11.8	46.8	0.526	0.2	0.3	0.4
1 (DC-81)	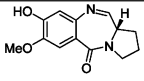	NA	NA	NA	NA	0.1[e]	0.2[e]	0.3[e]
4 (SJG-136)[f]	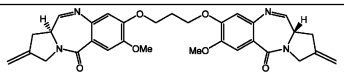	0.0074	0.0871	0.562	0.0038	16.1[g]	18.2[g]	20.5[g]

[a] For CT-DNA alone, ΔT_m = 67.44 ± 0.07 °C (mean from >80 experiments). All ΔT_m values are ± 0.1−0.2 °C. [b] For a fixed 1:10 molar ratio of [ligand]/[DNA], DNA concentration = 50 μM (bp) (i.e., 100 μM in DNAp) and ligand concentration = 5 μM, in aqueous sodium phosphate buffer [10 mM sodium phosphate + 1 mM EDTA, pH 7.00 ± 0.01]. [c] Value of 21.5 °C determined after incubation for 72 h. [d] Value of 19.2 °C determined after incubation for 72 h. [e] Values of 0.3, 0.5, 0.7, and 0.8 °C were determined for **1** at a higher 1:5 molar ratio after incubation for 0, 4, 18, and 72 h, respectively. [f] Values of 10.2, 13.1, 15.1, and 15.5 °C were determined for DSB-120 at a higher 2:5 [ligand]/[DNA(bp)] molar ratio after incubation for 0, 4, 18, and 72 h, respectively.[30,31,52] [g] Values of 21.3/25.7, 25.1/31.9, 28.3/33.6, and 29.4/34.4 °C were determined for **4** at higher 1:5/2:5 molar ratios after incubation for 0, 4, 18, and 72 h, respectively.[33] NA = Not available.

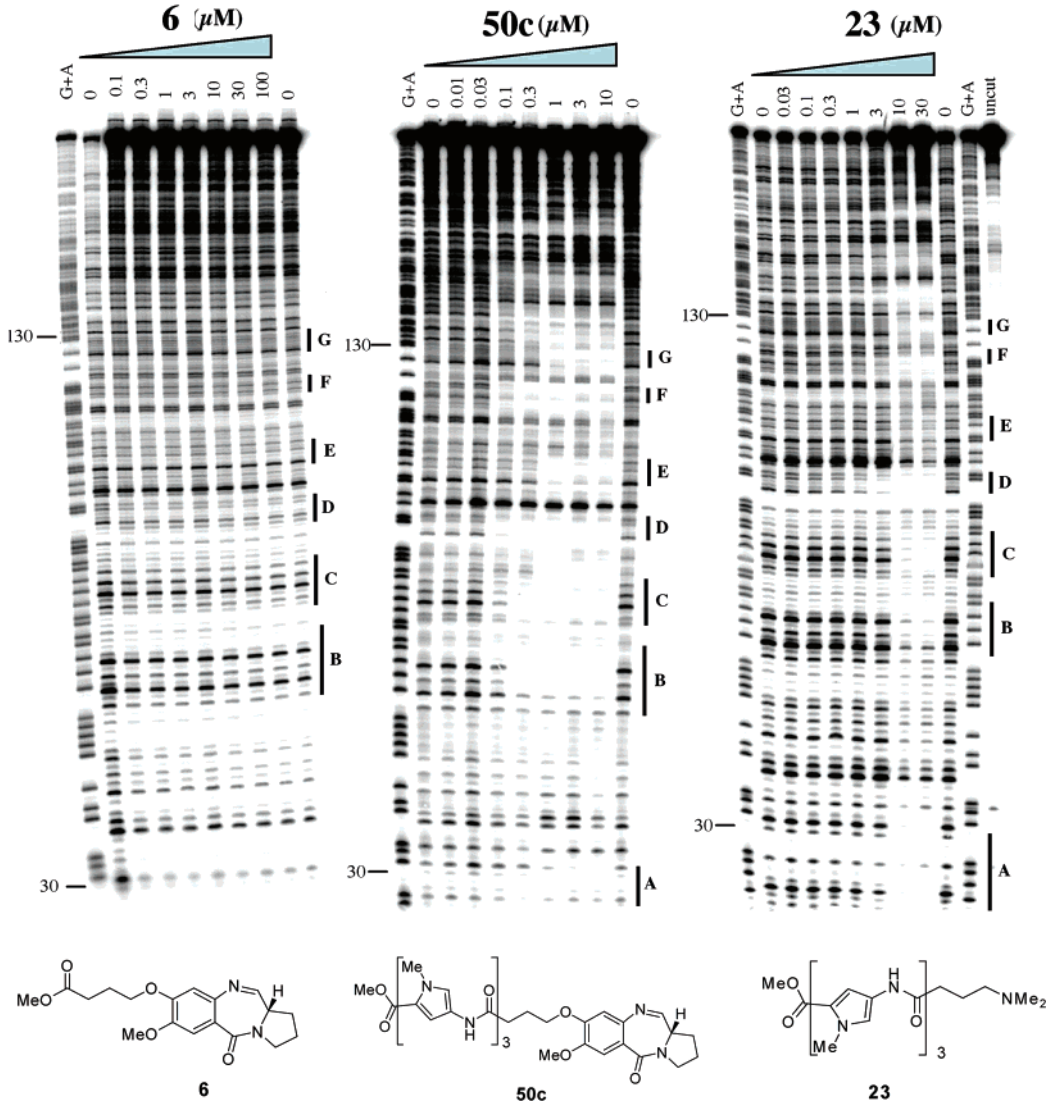

Figure 4. DNase I footprinting gels showing the binding profiles of **6** (left), **50c** (center), and **23** (right) on forward-labeled MS2 DNA. Differential Cleavage Plots for both this fragment (between positions 30−130) and the reverse fragment (between positions 130−230; not indicated) are shown in Figure 5. "G + A" represents a standard Maxim-Gilbert purine marker lane, and 'Uncut' represents DNA not treated with DNase I. The lettering system and vertical bars refer to the footprinted regions on the forward fragment as identified in the legend to Figure 5.

(Supporting Information). However, not all 5′-PuGPu-3′ sequences were footprinted, suggesting that local sequence and structure are crucial factors in determining the overall sequence-selectivity of these agents. The comparison of control molecule **6** to anthramycin in these footprinting experiments indicates the importance of C2−C3 unsaturation and C2-substitution in enhancing the DNA-binding reactivity.[41,42]

Conjugate **38** (the predecessor to **50c** and containing only three carbon atoms in the linkage between the PBD and polypyrrole tail) was also assessed for DNA binding by DNase I footprinting (S5, Supporting Information). The results confirm the predictions from molecular modeling and the indication from T_m studies that **38** should have a poorer fit in the DNA minor groove compared to **50c** and thus a lower reactivity toward DNA. The gel provided in S5 shows that for **38** footprints first appear at ~3 μM which is 30-fold higher than the concentration at which footprints first appear for **50c** (~0.1μM; see Figure 4). Furthermore, differential cleavage analysis (Supporting Information, S6) shows, as expected, that the actual pattern of footprints produced by **38** is similar to **50c**, although there are a few differences such as K and L (footprints that are weaker or lacking for **38**). Also, comparing the images (Figures 5 and S6) there are distinct differences at positions M and G at which compound **38** does not footprint.

Taking all of these data into account (e.g., see legend to Figure 5), the majority of these sites conform to a consensus motif (5′-XGXW$_z$, $z = 3 \pm 1$; W = A or T; X = any base but preferably a purine) that correlates well with the already established individual sequence-selective preferences of both the PBD and polypyrrole components. Eleven of the thirteen sites conform to this consensus motif as follows (reactive GC base pair underlined): 5′-^{20}TGATTACGA^{28}-3′, 5′-^{50}ATCCATATGCG^{60}-3′, 5′-^{62}CAATACACA^{70}-3′, 5′-^{77}ATTTCCA^{83}-3′, 5′-^{109}GGTTAA^{114}-3′, 5′-^{124}CTATC^{128}-3′, 5′-^{136}AGCAATTAGGG^{146}-3′, 5′-^{156}TTATGTAAAGTACG^{169}-3′, 5′-^{182}TGTTTTGTCAT^{192}-3′, 5′-^{201}CGAATGCGGAT^{211}-3′ and 5′-^{234}ATGCAAGCTT^{243}-3′), while the other two do not (5′-^{90}CTAGTCG^{96}-3′ and 5′-^{216}TAGAGT^{221}-3′).

In Vitro Transcription Assay. Conjugate ligands **50a**−**f** were subjected to an in vitro transcription assay[40] to establish whether any could inhibit transcription. As with the DNase I footprinting results, each member produced similar T-stop patterns. Results for **50c** and **50a**,**b**,**d**−**f** are shown in Figure 6 and S7 of Supporting Information, respectively. It should be

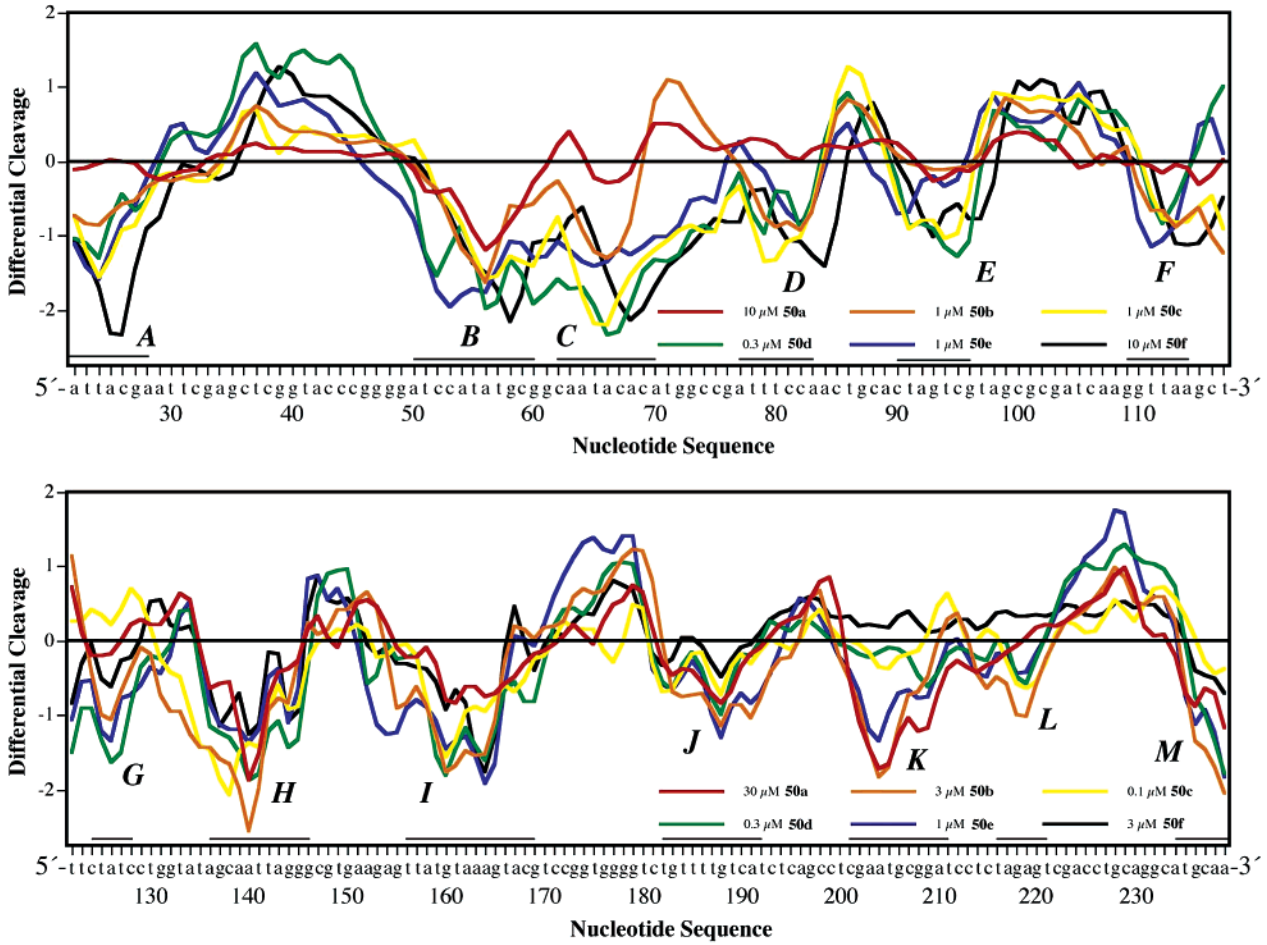

Figure 5. Differential Cleavage Plots showing the DNase I footprinting profiles of **50a**−**f** for the forward (A−G) and reverse (H−M) strands. Approximate positions of footprints are annotated with horizontal black bars: A: 5′-^{20}TGATTACGA^{28}-3′; B: 5′-^{50}ATCCATATGCG^{60}-3′; C: 5′-^{62}CAATACACA^{70}-3′; D: 5′-^{77}ATTTCCA^{83}-3′; E: 5′-^{90}CTAGTCG^{96}-3′; F: 5′-^{109}GGTTAA^{114}-3′; G: 5′-^{124}CTATC^{128}-3′; H: 5′-^{136}AGCAATTAGGG^{146}-3′; I: 5′-^{156}TTATGTAAAGTACG^{169}-3′; J: 5′-^{182}TGTTTTGTCAT^{192}-3′: K: 5′-^{201}CGAATGCGGAT^{211}-3′; L: 5′-^{216}TAGAGT^{221}-3′; M: 5′-^{234}ATGCAAGCTT^{243}-3′. Note that the concentrations of drugs used are different in the top and bottom panels. However, in every experiment the concentration was above the approximate IC_{50} value for each compound.

noted that the intensities of the T-stops are proportional to their radiolabeled cytidine content. All seven observed T-stops localize within a few bases of prominent footprints produced by the same compounds, and the correlation is highlighted in Figure 7 where the T-Stops are depicted as asterisks. Those with transcript lengths in nucleotides (sequence position in brackets) of 55 (51), 64 (60), 95 (91), 111 (107) and 142 (138) nucleotides are found on the 5'-side of the likely binding sites. The two remaining T-stops, 87 (8) and 132 (128), are located only one or two base pairs to the 3′-side of the nearest footprint.

In general, all compounds provide T-stops within the same concentration range, producing 50% inhibition of full-length transcript synthesis at around 5 μM (for comparison, SJG-136 requires a dose of 1−2 μM[40]). However, the use of this particular assay in determining, or even estimating, affinity constants has not been validated and therefore only sequence data can be analyzed. Although **6** did not produce any footprints at concentrations up to 100 μM, its efficacy in the *in vitro* transcription assay was assessed as it is known that this assay is more sensitive than footprinting.[40] Figure 6 shows that control PBD **6** is able to inhibit RNA production, although at concentrations approximately 10-fold higher than **50c** (i.e. first T-stops appearing at 1.5μM vs 0.15μM, respectively). By comparison, **3** (anthramycin) provides a robust blockade to viral RNA polymerase with several intense T-stops appearing at concentrations as low as 0.005 μM (S8, Supporting Information). In addition to the T-stops observed in S8, there is evidence of much weaker sites at 95, 100, 111, and 122 nucleotides. The most intense T-stops (lengths 55, 87, 128, 132, 205, 220, and 231 corresponding to positions 51, 83, 124, 128, 201, 216, and 227, respectively) are all located either 5'- to or within the closest footprinted site (55 − *B*, 87 − *D*, 128 − *K*, 132 − *L*, 205 − *R*, 220 − *U*, 231 − *W*; lettered according to Figure 4). Interestingly, these are all 5′-PuGPu-3′ sites with no bias toward the upper or lower strand. The less-favored 5′-PyGPu-3′ sites do not immediately appear to be associated with any T-stops.

It is interesting that **6** does not prevent full-length transcript production to the same extent as either the **50a**−**f** conjugates or **3**. For example, at 50 μM of **6** there is very little change in the amount of 266-nt product, whereas complete inhibition occurs at ∼5 μM anthramycin (Figure S8) and <15 μM **50c** (Figure 6). Also, **6** produces T-stops at identical sites to anthramycin, but many others in addition. These extra T-stops include a mixture of 5′-Pu**G**Pu-3' sites (5′-^{108}A**G**G^{110}-3′ and 5′-^{192}TCT^{194}-3′ [5′-A**G**A-3′ on the complementary strand]), two 5′-Pu**G**Py-3′ (5′-^{72}G**G**C^{74}-3′ and 5′-^{92}A**G**T^{94}-3′) and what are most likely to be 5′-Py**G**Py-3′ sites (5′-^{66}ACA^{68}-3′ [5′-TGT-3′ on the lower strand], 5′-^{86}T**G**C^{88}-3′ and 5′^{95}C**G**T^{97}-3′). The finding that **50c** is able to block transcription at a 10-fold lower concentration than the PBD unit (**6**) alone (i.e. significant stops first appear at 0.5 μM and 5 μM for **50c** and **6**, respectively),

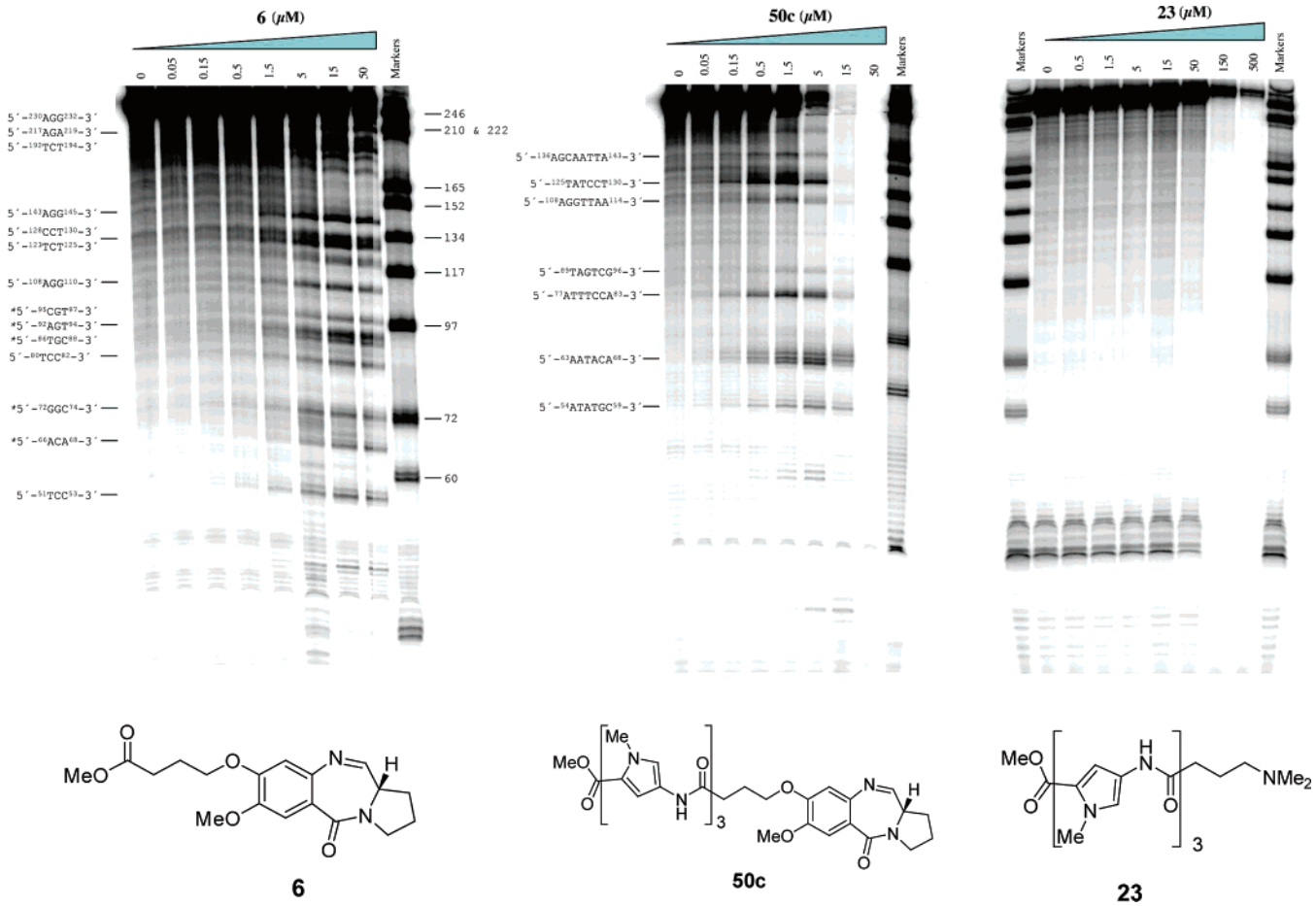

Figure 6. Inhibition of viral T7 RNA polymerase-catalyzed transcription by **6** (left), **50c** (center), and **23** (right). The nearest likely binding sites corresponding to robust T-stops are indicated to the left of each gel. The full-length fragment contains 266 nt, and the 'marker' lanes show the length (in nucleotides) of the enzymatically created markers which are identical for all three gels. The presence of a 60 nucleotide marker and the absence of a 56 nucleotide marker (as present in Figures S7A−E in Supporting Information) is due to the use of an alternative enzyme (see Experimental Section of main text). Note that **23** fails to block transcription as it binds noncovalently to DNA.

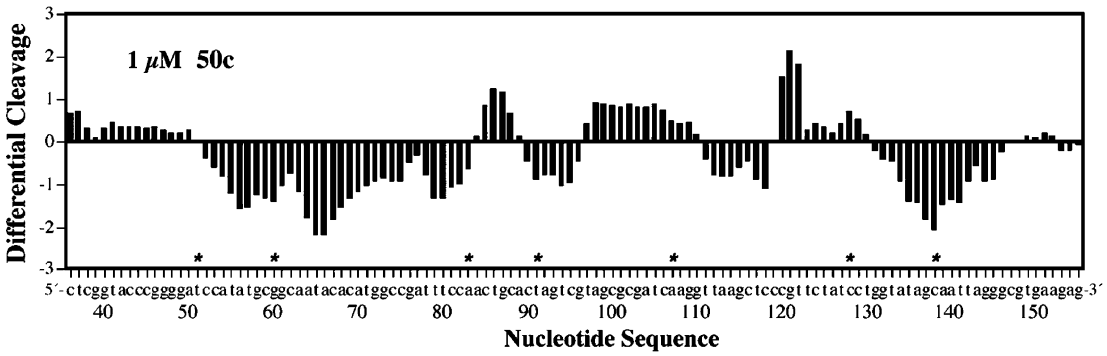

Figure 7. Differential cleavage analysis of **50c** (1 μM) on the central base portion (positions 40−150) of the MS2 fragment. Vertical bars represent the extent of cleavage at each nucleotide compared to control. Positive and negative deflections indicate enhanced and reduced DNase I cleavage, respectively. Negative deflections are indicative of regions protected by the bound drug. The positions of the T-stops derived from Figure 6 are indicated by asterisks.

suggests that the polypyrrole part of the conjugate **50c** is driving the reaction with DNA.

As anticipated, given its noncovalent interaction with DNA, **23** is unable to produce sequence-selective T-stops at concentrations of up to 500 μM. However, production of the full-length transcript does reduce as the concentration of **23** increases from 0.5 μM to 500 μM which is thought to be due to concentration-dependent binding of **23** to the T7 promoter sequence which gradually inhibits the RNA polymerase from binding. In accordance with the DNase I footprinting data, **38** produces T-stops at identical positions to **50a**−**f** (data not shown) with one exception; the lack of a T-stop corresponding to the 132-nt transcript which corresponds well with the lack of footprinting around this site by **38**. The range of concentrations over which **38** exerts its effect is similar to that of **50c**, however, the use of this assay to compare effective concentration ranges has not been validated.

In Vitro Cytotoxicity. Conjugates **50a**−**f** were all significantly cytotoxic across the cell lines studied and, although there is not a perfect correlation with the thermal denaturation data, those compounds with the highest ΔT_m values (**50c**−**e**) have the lowest average TGI and LC_{50} values across the 60 cells

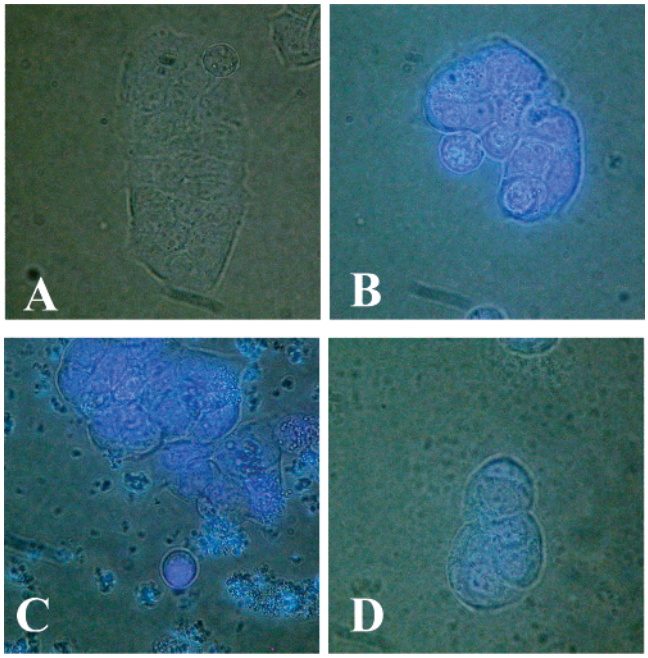

Figure 8. Nuclear uptake of conjugates following incubation with MCF-7 cells for 24 h at 100 μM. A: Drug-free control, B: **50a**, C: **50c**, D: **50f**.

lines of the NCI 60 panel. It is significant that, despite its high molecular weight (i.e., 1079), **50f** is still highly cytotoxic. The activity appears to fall off slightly for **50b** although it is particularly potent in K562 (7.1 nM). **50a** is the least potent member of the series, although it still significantly active across all cell lines. Conjugate **38** with the three-carbon linker is less cytotoxic than any of the **50a**−**f** series which was anticipated from the modeling and DNA thermal denaturation data.

As anticipated from the thermal denaturation, footprinting and in vitro transcription data, the control polypyrroles **22** and **23** were relatively noncytotoxic with IC_{50} values of >10 μM. Similarly, the PBD control molecule **6** was significantly less cytotoxic (e.g., IC_{50} = 0.526 μM in K562 cells) compared to **50a**−**f**, as was the control PBD dilactam **56** (IC_{50} >10 μM in K562). Taken together, these results further illustrate the synergy of joining a PBD unit to the polypyrrole fragments whereby the combination provides dramatically enhanced cytotoxicity and DNA-binding affinity compared to the component units alone. Another interesting finding is that **50a**−**f** are significantly more cytotoxic than the conjugates reported by Baraldi and Lown, with the possible exception of **12d** (n = 4) which has a reported IC_{50} of 0.04 μM in K562 cells.[10] One possible conclusion from these studies is that the positively charged 3-(dimethylamino)propyl and amidino termini of the earlier conjugates reduce their cellular penetration efficiency compared to the neutral esters reported here.

Cellular and Nuclear Penetration. The preliminary data reported here indicate that, at the highest drug concentrations used and an exposure time of 24 h, it is clear that all compounds are taken up into MCF-7 cells. Cellular uptake was evident for all conjugates at a concentration of 100 μM, with particularly strong nuclear fluorescence observed for **50a**−**c.** The fluorescence appeared more diffuse throughout the cell for the longer conjugates **50d**−**f**, suggesting poorer nuclear penetration. Furthermore, the length of the molecules appeared to have an effect on their rate of uptake, with **50a** being taken up very rapidly (<1 h) but longer members (**50b** and **50c**) detectable only after 3 h. Representative images from these experiments are shown in Figure 8. Although high concentrations of conjugates were used in these preliminary experiments, this did not appear to be detrimental to the cells which, over a 24 h period, remained attached while maintaining a similar morphology to drug free controls.

Conclusions

The systematic studies of the PBD-pyrrole conjugates **50a**−**f** (together with the appropriate control molecules) using molecular modeling, thermal denaturation, DNA footprinting, in vitro transcription stop assays, confocal microscopy, and cytotoxicity evaluations show that a four-carbon linkage is markedly superior to a three-carbon one. This separation between the C8-position of the PBD and the *N*-terminal of the first heterocycle was first suggested by Lown to be preferable to the three-carbon link used by Baraldi in terms of maximizing DNA-binding efficacy. The superiority of the four-carbon link in improving the isohelical fit of the molecules in the minor groove can now be explained by molecular modeling. Furthermore, based on the higher cytotoxicity values for members of the **50a**−**f** series compared to the Lown and Baraldi conjugates it appears that, although high cytotoxicity is achievable with 3-(dimethylamino)-propyl or amidino termini, a methyl ester terminus is preferable. This may be due to greater cellular and/or nuclear penetration by the ester derivatives. Further advantages of the methyl ester compounds are that they can be isolated in the N10−C11 imine form and do not appear to suffer from the insolubility problem experienced with the 3-(dimethylamino)propyl-terminated conjugates, an issue that prompted the development of glycosylated analogues (i.e., **13a**−**h** in Figure 2) which had improved water solubility but poorer IC_{50} values (in the 0.6 to 100 μM range) along with inherent synthetic challenges. The fact that **38** and **50a**−**f** can be isolated as N10−C11 imines appears to be due solely to the ester moiety, as earlier conjugates differ mainly in this aspect. The Lown conjugates all have a 3-(dimethylamino)-propyl terminus which presumably raises polarity when protonated, thus inhibiting cellular penetration and reducing cytotoxic potency.

The results of this study also highlight the remarkable synergy of joining a PBD unit to a polypyrrole fragment in terms of DNA reactivity, helix stabilization (T_m values), and cytotoxicity. The DNA footprinting and in vitro transcription studies demonstrate that conjugates **50a**−**f** take on the properties of both component fragments in terms of targeting a run of A/T base pairs (through the polypyrrole fragment) adjacent to a Pu-**G**-Pu site which becomes alkylated by the PBD. Unexpectedly, all six members (**50a**−**f**) were found to bind, for the most part, to similar sequences within the MS2 fragment. The majority of these sites conformed to a consensus motif (5'-XGXW$_z$, z = 3 ± 1; W = A or T; X = any base but preferably a purine) that correlated well with the individual established sequence-selective preferences of the PBD and polypyrrole components. The data indicate that a molecule containing three or four *N*-methylpyrrole rings is optimal for DNA stabilization and that a four-carbon rather than a three-carbon linker between the PBD and *N*-terminus of the first polypyrrole is preferable. There also appears to be a correlation between the overall length of the binding site and the molecular length of the hybrid conjugate.

The in vitro transcription studies show that all six conjugates **50a**−**f** efficiently inhibit transcription at sites that mostly correspond to the DNA footprints, and that the PBD subunit is critical for realizing this. The addition of a polypyrrole fragment to a PBD subunit significantly reduces the number of adducts

formed on the MS2 fragment, thus indicating an increase in sequence-selectivity compared to a simple PBD monomer. However, the fact that **50c** is able to block transcription at a 10-fold lower concentration than the PBD unit (**6**) alone suggests that the polypyrrole part of the conjugate **50c** is driving the reaction with DNA.

Overall, the PBD−polypyrrole conjugates **50a**−**f** show characteristics highly desirable for gene-targeting purposes, including the ability to be isolated in the N10−C11 imine form, adequate water solubility and cellular/nuclear penetration characteristics, sequence-selective DNA binding with surprisingly high affinity, and the ability to robustly block RNA transcription at well-defined sequences. Further work is underway to establish the structure of the DNA adducts being formed, and the possible consequences of hydrolysis of the methyl ester termini in vivo. Versions of **50a**−**f** containing alternative non-pyrrole heterocyclic units and extended analogues of greater length are also being evaluated. Results from these studies will be reported in due course, together with in vivo data for selected compounds.

Experimental Section

Molecular Modeling. Initial models for **38** and **50c** were built using InsightII (Biosym Inc., San Diego, CA). For parametrization purposes the molecules were divided into fragments: the terminal methoxy group, the pyrrole unit, and the PBD (including the linker). Each fragment was capped with methylamino and/or acetyl groups as appropriate and geometry-optimized at the HF/6-31G* level using Gaussian98.[43] All further molecular modeling was performed using programs from the Amber7 suite[44] running on Silicon Graphics workstations. Partial charges for the fragments were calculated using the RESP procedure.[45] Missing force field parameters were estimated from the optimized geometry or by analogy to similar parameters in the parm99 database.[46] Molecular mechanics energy minimizations on the capped fragments were used to check that the ab initio geometries were maintained. The molecular model for the 17-mer DNA target sequence 5′-TTTTGCAAAAAGCT-TCA-3′, found to be a favored site for binding in early footprinting studies (results not shown) was built in standard B-form geometry using the Amber program Nucgen (covalently modified guanine underlined). Alternative DNA sequences were not investigated because, although DNA helical parameters are sequence dependent, the range of variation is small compared to what would be required to qualitatively alter the conclusion regarding the relative isohelicity of the two ligands. Thus a quantitative analysis of sequence-dependent effects was not carried out.

Initial docking of **38** and **50c** to the minor groove of the target DNA was performed manually. The PBD unit was oriented appropriately (i.e., A-ring toward the 3′-end of the covalently bound strand[5] and the pyrrole units residing within the A_5 tract) for attack by the exocyclic C2-amino group of guanine-5 (underlined) on the N10−C11 imine function of the PBD. The torsion angles in the linker and between the pyrrole units were adjusted to obtain, as far as possible, an isohelical conformation with the DNA. Energy minimizations and molecular dynamics simulations on the complex were performed using the Generalized Born solvation model.[47] The protocol consisted of: initial energy minimization of the ligand alone; 10 ps MD on the complex gradually warming to 300 K with position restraints of 10 kcal·mol^{-1}·Å^{-2} on the DNA; then three more 10 ps MD simulations at 300 K with restraints on the DNA reduced to 5, then 2.5, then 1 kcal·mol^{-1}·Å^{-2}. The final 'production' MD run was for 100 ps, maintaining the 1 kcal·mol^{-1}·Å^{-2} restraint on DNA atoms. Energetic analysis of the MD run was performed using the MM-GBSA module[19] of Amber.[48]

Chemistry. General. Melting points (mp) were obtained using a Gallenkamp melting point apparatus and are uncorrected. IR spectra were measured using a Mattson 2020 Galaxy Series FT-IR spectrometer. ^{1}H and ^{13}C NMR spectra were acquired using a Brüker Avance 400 spectrometer at 400 and 100 MHz, respectively. Mass spectra were recorded with a Micromass Platform Spectrometer or an AEI MS-902 spectrometer using the electrospray ionization technique. Flash column chromatography refers to medium-pressure silica gel (C60, 40−60 μm) preparative column chromatography. Procedures for the synthesis of intermediates **16**, **17**, **19**, **20**, **24**, **26**, **28**, **31**, **32**, **40**-**45**, **52**−**54** are provided in Supporting Information (S9). ^{13}C NMR and IR data for compounds **6**, **22**, **35**, **38**, **46**−**48**, and **50a**−**f** are provided in Supporting Information (S10). Compounds **18**, **21**, **25**, **27**, and **29** were formed in situ and used directly in the next step.[22−24] New compounds were judged to be pure for testing by analysis of their NMR, HRMS, and LCMS/HPLC data (summarized in Supporting Information, S11).

Methyl 4-({4-[(4-Formamino-1-methyl-1*H*-pyrrole-2-carbonyl)amino]-1-methyl-1*H*-pyrrole-2-carbonyl}amino)-1-methyl-1*H*-pyrrole-2-carboxylate (22). The Boc pyrrole trimer **19** (0.1 g, 0.20 mmol) in a dry round-bottomed flask was treated with 4M HCl in dioxane (2 mL). The reaction mixture was stirred for 30 min during which time a precipitate formed. The solvent was then removed and the residue dried in vacuo. The residue was dissolved in anhydrous CH_2Cl_2 (2 mL) then the formic acid (0.014 g, 0.41 mmol, 2.0 equiv) was added followed by EDCI (0.153 g, 0.80 mmol, 4.0 equiv) (effervescence observed) and DMAP (0.122 g, 1.00 mmol, 5.0 equiv). The reaction mixture was stirred for 18 h then diluted with EtOAc (20 mL) and washed with 1M HCl solution (2 × 15 mL) then saturated $NaHCO_3$ solution (3 × 15 mL). The organic layer was dried ($MgSO_4$) and concentrated in vacuo to give an off white solid, **22** (0.051 g, 60%). ^{1}H NMR (d_6-acetone) δ 9.23 (1H, s, NCH_3), 9.20 (1H, s, NH), 9.04 (1H, s, NH), 8.20 (1H, d, J = 1.6 Hz, CHO), 7.49 (1H, d, J = 2.0 Hz, Py-H), 7.21 (1H, d, J = 1.9 Hz, Py-H), 7.18 (1H, d, J = 1.9 Hz, Py-H), 6.97 (1H, d, J = 1.9 Hz, Py-H), 6.92 (1H, d, J = 2.0 Hz, Py-H), 6.82 (1H, d, J = 1.9 Hz, Py-H), 3.94 (3H, s, O/NCH_3), 3.91 (3H, s, O/NCH_3), 3.76 (3H, s, OCH_3); MS (ES$^+$) m/z (relative intensity) 427 ([M + H]$^+$•, 100%); Acc. Mass $C_{20}H_{22}N_6O_5$ calc. 427.1725 found 427.1713.

Methyl 4-[(4-{[4-(4-Dimethylaminobutyrylamino)-1-methyl-1*H*-pyrrole-2-carbonyl]amino}-1-methyl-1*H*-pyrrole-2-carbonyl)-amino]-1-methyl-1*H*-pyrrole-2-carboxylate (23).[21] The Boc pyrrole trimer **19** (0.1 g, 0.20 mmol) in a dry round-bottomed flask was treated with 4M HCl in dioxane (2 mL). The reaction mixture was stirred for 30 min during which time a precipitate formed. The solvent was then removed and the residue dried in vacuo. The residue was dissolved in anhydrous DMF (1 mL) and *N*,*N*-dimethylaminobutyric acid (0.026 g, 0.20 mmol, 1.0 equiv) was added followed by EDCI (0.096 g, 0.50 mmol, 2.5 equiv) then DMAP (0.048 g, 0.40 mmol, 2.0 equiv). The reaction mixture was stirred for 96 h then the solvent was removed in vacuo. The residue was diluted with water (10 mL) and extracted with EtOAc (4 × 5 mL). The combined organic layers were dried ($MgSO_4$) and concentrated in vacuo to give a solid which was suspended in Et_2O (10 mL). Collection of the precipitate and vacuum-drying gave **23** as a solid (0.082 g, 81%). ^{1}H NMR (d_6-DMSO) δ 9.91 (1H, s, NH), 9.89 (1H, s NH), 9.81 (1H, s, NH), 7.47 (1H, d, J = 1.9 Hz, Py-H), 7.23 (1H, d, J = 1.8 Hz, Py-H), 7.16 (1H, d, J = 1.8 Hz, Py-H), 7.06 (1H, d, J = 1.8 Hz, Py-H), 6.91 (1H, d, J = 1.9 Hz, Py-H), 6.87 (1H, d, J = 1.9 Hz, Py-H), 3.85 (3H, s, NCH_3), 3.84 (3H, s, NCH_3), 3.83 (3H, s, NCH_3), 3.75 (OCH_3), 2.33−2.24 (4H, 2 × t, J = 7.3 Hz, side-chain H-2,4), 2.20 (6H, s, N[CH_3]$_2$), 1.72 (2H, p, J = 7.3 Hz, side-chain H-3).

3-[5-Amino-4-((2*S*)-2-hydroxymethyl-pyrrolidine-1-carbonyl)-2-methoxyphenoxy]propionic Acid Benzyl Ester (33). Nitro compound **32** (59 g, 0.128 mol) was dissolved in MeOH (650 mL). Tin(II) chloride dihydrate (130 g, 0.577 mol, 4.5 equiv) was added, and the mixture was heated under reflux for 6 h. The solvent was removed in vacuo, and the residue was dissolved in EtOAc (1 L) in a 5 L flask, and saturated $NaHCO_3$ solution (2 L) was added carefully. The mixture was stirred for 2 h, and the resulting emulsion (pH 8) was left to settle overnight then filtered through Celite. The Celite pad was washed twice with EtOAc and the aqueous layer extracted with further EtOAc. The organic layers were combined, dried ($MgSO_4$), and concentrated in vacuo to give crude **33** as a black tar (50 g). The product was used in the next step with no

further purification. ^{1}H NMR ($CDCl_3$) δ 7.40−7.32 (5H, m, benzyl), 6.74 (1H, s, phenyl H-3), 6.28 (1H, s, phenyl H-6), 5.19 (2H, s, benzyl CH_2), 4.33−4.23 (3H, m, side-chain H-1, pyrrolidine H-2), 3.73 (3H, s, OCH_3), 3.77−3.50 (4H, m, pyrrolidine H-5, CH_2−OH), 2.91 (2H, t, J = 6.2 Hz, side-chain H-2), 2.20−2.10 (1H, m, pyrrolidine H-3), 1.88−1.60 (3H, m, pyrrolidine H-3,4).

3-[5-*tert*-Butoxycarbonylamino-4-((2*S*)-2-hydroxymethylpyrrolidine-1-carbonyl)-2-methoxy-phenoxy]propionic Acid Benzyl Ester (34). Crude amine **33** (39 g, 52.3 mmol) was dissolved in THF (650 mL), and di-*tert*-butyl dicarbonate (22.4 g, 0.103 mol) was added in one portion. The mixture was heated under reflux for 18 h, after which TLC (EtOAc) showed completion of the reaction. The volatiles were removed in vacuo, and the residue was dissolved in EtOAc (500 mL) and washed with water (2 × 200 mL) and brine (200 mL). After drying ($MgSO_4$) and concentration in vacuo, crude **34** was obtained as a brown foam (53.2 g) slightly contaminated with *tert*-butyl alcohol and solvent. This material was used in the next step without further purification. ^{1}H NMR ($CDCl_3$) δ 8.41 (1H, br s, NH), 7.82 (1H, s, phenyl H-6), 7.38−7.30 (5H, m, benzyl), 6.81 (1H, s, phenyl H-3), 5.18 (2H, s, benzyl CH_2), 4.44−4.34 (3H, m, pyrrolidine H-2, side-chain H-1), 3.76 (3H, s, OCH_3), 3.77−3.47 (4H, m, pyrrolidine H-5, CH_2−OH), 2.93 (2H, t, J = 6.2 Hz, side-chain H-2), 2.10−2.00 (1H, m, pyrrolidine H-3), 1.88−1.60 (3H, m, pyrrolidine H-3,4), 1.50 (9H, s, C[CH_3]$_3$).

(11*S*,11a*S*)-8-(2-Benzyloxycarbonylethoxy)-11-hydroxy-7-methoxy-5-oxo-2,3,11,11a-tetrahydro-1*H*,5*H*-pyrrolo[2,1-*c*][1,4]benzodiazepine-10-carboxylic Acid *tert*-Butyl Ester (35). The crude Boc amine **34** (50 g, 0.094 mol) was dissolved in anhydrous CH_2Cl_2 (500 mL) at room temperature under N_2. 4 Å molecular sieves (47 g) and pyridinium dichromate (43 g, 0.114 mol, 1.2 equiv) were added, and the mixture was stirred for 4 h. Once the initial exotherm had subsided, the mixture was sampled by TLC. Upon completion of the reaction, EtOAc (1 L) was added with stirring. The black mixture was filtered through Celite, and the residue was mixed with warm EtOAc (3 × 200 mL) and refiltered. Evaporation of the combined organic phase gave a black foam which was subjected to column chromatography (EtOAc−petroleum ether, 70/30 v/v) to give **35** as a pink-colored foam (16 g). Further fractions gave 2 g of additional product (27% yield, 3 steps). $[\alpha]^{25}_D$ = +335° (c = 0.212, $CHCl_3$); ^{1}H NMR ($CDCl_3$) δ 7.37−7.29 (5H, m, benzyl PhH), 7.22 (1H, s, H-6), 6.66 (1H, s, H-9), 5.55 (1H, d, J = 6.4 Hz, H-11) 5.18 (2H, s, benzyl CH_2), 4.40−4.23 (2H, m, side-chain H-1), 3.88 (3H, s, OCH_3), 3.76−3.44 (4H, m, H-3,11a, OH), 2.93 (2H, t, J = 6.7 Hz, side-chain H-2), 2.14−1.98 (4H, m, H-1,2), 1.36 (9H, s, C[CH_3]$_3$); MS (ES^+) m/z (relative intensity) 527 ([M + H]$^{+\bullet}$, 30%), 471 (50%), 409 (100%).

(11*S*,11a*S*)-8-(2-Carboxyethoxy)-11-hydroxy-7-methoxy-5-oxo-2,3,11,11a-tetrahydro-1*H*,5*H*-pyrrolo[2,1-*c*][1,4]benzodiazepine-10-carboxylic Acid *tert*-Butyl Ester (36).[27] Benzyl ester **35** (9 g, 17.1 mmol) was dissolved in EtOH (120 mL), and a slurry of 10% Pd/C (0.5 g) in EtOH was added. The mixture was hydrogenated in a Parr apparatus at 16 psi until the H_2 uptake ceased (2 h). The reaction mixture was filtered through Celite and the residue washed with EtOH. The solvent was removed in vacuo to give **36** as a white foam (quantitative yield). $[\alpha]^{24.9}_D$ = +104° (c = 0.920, $CHCl_3$) ^{1}H NMR (d_6-DMSO) δ 7.24 (1H, s, H-6), 6.68 (1H, s, H-9), 5.60 (1H, d, ;= 10.0 Hz, H-11), 4.31 (2H, t, J = 7.5 Hz, side-chain H-1), 3.90 (3H, s, OCH_3), 3.76−3.44 (3H, m, H-3,11a), 2.92 (2H, t, J = 6.2 Hz, side-chain H-2), 2.14−1.98 (4H, m, H-1,2), 1.38 (9H, s, C[CH_3]$_3$). Based on the ^{1}H NMR and the method employed, the product was found to be identical to the literature description.[27]

(11*S*,11a*S*)-11-Hydroxy-7-methoxy-8-(3-{5-[5-(5-methoxycarbamoyl)-1-methyl-1*H*-pyrrol-3-ylcarbamoyl)-1-methyl-1*H*-pyrrol-3-ylcarbamoyl]-1-methyl-1*H*-pyrrol-3-ylcarbamoyl}-ethoxy)-5-oxo-2,3,11,11a-tetrahydro-1*H*,5*H*-pyrrolo[2,1-*c*][1,4]benzodiazepine-10-carboxylate *tert*-Butyl Ester (37). The Boc pyrrole trimer **19** (0.16 g, 0.32 mmol) in a dry round-bottomed flask was treated with 4M HCl in dioxane (2.5 mL). The reaction mixture was stirred for 30 min during which time a precipitate formed. The solvent was then removed and the residue dried in vacuo. The residue was dissolved in anhydrous DMF (2.5 mL) then the Boc-PBD acid **36** (0.139 g, 0.32 mmol, 1 equiv) was added followed by EDCI (0.122 g, 0.64 mmol, 2.0 equiv) and DMAP (0.096 g, 0.80 mmol, 2.5 equiv). The reaction mixture was stirred for 18 h then diluted with EtOAc (40 mL) and washed with 10% citric acid solution (3 × 50 mL) then saturated $NaHCO_3$ solution (3 × 50 mL). The organic layer was dried ($MgSO_4$) and concentrated in vacuo to give a foamy solid, **37** (0.170 g, 65%). ^{1}H NMR (d_6-DMSO) δ 10.07 (1H, s, NH), 9.96 (2H, s, NH), 7.49 (1H, d, J = 1.8 Hz, Py-H), 7.26 (1H, d, J = 1.6 Hz, Py-H), 7.21 (1H, d, J = 1.6 Hz, Py-H), 7.07 (1H, d, J = 1.6 Hz, Py-H), 7.06 (1H, s, H-9), 6.93 (1H, s, Py-H), 6.92 (1H, d, J = 1.8 Hz, Py-H), 6.76 (1H, s, H-6), 6.46 (1H, bs, OH), 5.47−5.41 (1H, m, H-11), 4.30−4.16 (2H, m, side-chain H-1), 3.85 (6H, s, O/NCH_3), 3.78 (3H, s, O/NCH_3), 3.76 (3H, s, O/NCH_3), 3.74 (3H, s, O/NCH_3), 3.49−3.36 (1H, m, H-11a), 3.28−3.18 (2H, m, H-3), 2.80−2.77 (2H, m, side-chain H-2), 2.03−1.90 (4H, m, H-1,2), 1.19 (9H, s, C[CH_3]$_3$).

(11a*S*) Methyl 4-{[4-({4-[4-(7-Methoxy-5-oxo-2,3,5,11a-tetrahydro-5*H*-pyrrolo[2,1-*c*][1,4]benzodiazepine-8-yloxy)propionylamino]-1-methyl-1*H*-pyrrole-2-carbonyl]amino)-1-methyl-1*H*-pyrrole-2-carbonyl]amino}-1-methyl-1*H*-pyrrole-2-carboxylate (38). The Boc-PBD conjugate **37** (0.053 g, 0.12 mmol) dissolved in a solution of 95% aq. TFA (2.5 mL) cooled to −10 °C. The reaction mixture was stirred at this temperature for 3 h then poured into a flask containing ice (∼20 g). The mixture was adjusted to pH∼8 by careful addition of saturated $NaHCO_3$ solution. The aqueous phase was extracted with chloroform (3 × 20 mL). The combined organic layers were dried ($MgSO_4$) and concentrated in vacuo to give a pale yellow foam, **38** (0.044 g, 96%). $[\alpha]^{26.3}_D$ = +89° (c = 0.027, $CHCl_3$); ^{1}H NMR d_6-DMSO (d_6-DMSO) δ 9.99 (1H, s, NH), 9.91 (1H, s, NH), 9.90 (1H, s, NH), 7.79 (1H, d, J = 4.4 Hz, H-11), 7.46 (1H, d, J = 1.8 Hz, Py-H), 7.33 (1H, s, H-9), 7.23 (1H, d, J = 1.8 Hz, Py-H), 7.20 (1H, d, J = 1.7 Hz, Py-H), 7.18 (1H, d, J = 1.7 Hz, Py-H), 7.05 (1H, d, J = 1.8 Hz, Py-H), 6.90 (1H, d, J = 1.7 Hz, Py-H), 6.88 (1H, s, H-6), 4.17−4.00 (2H, m, side-chain H-1), 3.84 (3H, s, O/NCH_3), 3.84 (6H, s, O/NCH_3), 3.79 (3H, s, O/NCH_3), 3.73 (3H, s, O/NCH_3), 3.69−3.57 (2H, m, H-3,11a), 3.45−3.35 (1H, m, H-3), 2.79−2.73 (2H, m, side-chain H-2), 2.29−2.21 (2H, m, H-1), 2.01−1.92 (2H, m, H-2); MS (ES^+) m/z (relative intensity) 699 ([M + H]$^{+\bullet}$, 100%); Acc. Mass $C_{35}H_{38}N_8O_8$ calc. 699.2885 found 699.2872.

(11*S*,11a*S*) 11-Hydroxy-7-methoxy-8-(3-methoxycarbonylpropoxy)-5-oxo-2,3,11,11a-tetrahydro-1*H*,5*H*-pyrrolo[2,1-*c*][1,4]-benzodiazepine-10-carboxylic Acid Allyl Ester (46).[29] Oxalyl chloride (17.87 g, 12.28 mL, 1.8 equiv) in anhydrous CH_2Cl_2 (200 mL) was cooled to −40 °C, and a solution of anhydrous DMSO (16.23 g, 16.07 mL, 3.6 equiv) in anhydrous CH_2Cl_2 (200 mL) was added dropwise over 2 h, maintaining the temperature below −37 °C. A white suspension formed then redissolved. The crude Alloc-protected amine **45** (26 g, 57.7 mmol) in anhydrous CH_2Cl_2 (450 mL) was added dropwise over 3 h maintaining the temperature below −37 °C. The mixture was stirred at −40 °C for a further 1 h. A solution of DIPEA (32.1 g, 43.2 mL, 4.3 equiv) in anhydrous CH_2Cl_2 (100 mL) was added dropwise over 1 h, and the reaction was allowed to warm to room temperature. The mixture was extracted with a concentrated aqueous solution of citric acid. (pH 2−3 after extraction). The organic phase was washed with water (2 × 400 mL) and brine (300 mL), then dried ($MgSO_4$). Solvent removal in vacuo gave a paste; column chromatography (EtOAc−petroleum ether, 70/30 v/v) gave **46** (17.0 g, 62%); $[\alpha]^{26}_D$ = +122° (c = 0.2, $CHCl_3$); ^{1}H NMR ($CDCl_3$) δ 7.23 (1H, s, H-9), 6.69 (1H, s, H-6), 5.72−5.88 (1H, m, allyl H-2), 5.57−5.68 (1H, m, H-11), 5.15 (2H, d, J = 12.9 Hz, allyl H-3), 4.69−4.43 (2H, m, allyl H-1), 4.00−4.13 (2H, m, side-chain H-1), 3.84−3.95 (4H, m, OCH_3, OH), 3.62−3.72 (4H, m, OCH_3, H-3), 3.58−3.45 (2H, m, H-3,11a), 2.53 (2H, t, J = 7.2 Hz, side-chain H-3), 2.18−1.94 (6H, m, side-chain H-2, H-1,2); MS (ES^+) m/z 449 (M + H, 100%).

(11*S*,11a*S*)-7-Methoxy-8-(3-methoxycarbonylpropoxy)-5-oxo-11-(tetrahydropyran-2-yloxy)-2,3,11,11a-tetrahydro-1*H*,5*H*-pyrrolo[2,1-*c*][1,4]benzodiazepine-10-carboxylic Acid Allyl Ester (47). A solution of dihydropyran (4.22 mL, 46.2 mmol) and

4-toluenesulfonic acid (catalytic quantity, 0.020 g) in EtOAc (30 mL) was stirred for 10 min. Ester **46** (2.0 g, 4.62 mmol) was then added in one portion, and the mixture was stirred for 2 h. The solution was diluted with EtOAc (70 mL) and washed with saturated aqueous $NaHCO_3$ (50 mL), followed by brine (50 mL). The organic layer was dried ($MgSO_4$), and the volatiles were removed under vacuum. The oily residue of **47** (2.38 g, 100%) was pure by TLC (EtOAc) and was used directly in the next step. ^{1}H NMR ($CDCl_3$) mixture (4:5) of diastereoisomers δ 7.24−7.21 (1H, s × 2, H-9), 6.88−6.60 (1H, s × 2, H-6), 5.89−5.73 (2H, m allyl H-2, H-11), 5.15−5.04 (2H, m, allyl H-3), 4.96−4.81 (1H, m, pyran H-2), 4.68−4.35 (2H, m, allyl H-1), 4.12−3.98 (2H, m, side-chain H-1), 3.98−3.83 (4H, m, OCH_3, H11a), 3.74−3.63 (4H, m, OCH_3, H-3), 3.60−3.40 (3H, m, pyran H-6, H-3), 2.56−2.50 (2H, m, side-chain H-3), 2.23−1.68 (6H, m side-chain H-2, H-1,2), 1.66−1.48 (6H, m, pyran H-3,4,5); MS (ES^+) *m*/*z* (relative intensity) 533 ([M + H]$^+$, 100%).

(11*S*,11a*S*)-8-(3-Carboxypropoxy)-7-methoxy-5-oxo-11-(tetrahydropyran-2-yloxy)-2,3,11,11a-tetrahydro-1*H*,5*H*-pyrrolo[2,1-*c*][1,4]benzodiazepine-10-carboxylic Acid Allyl Ester (48). Methyl ester **47** (2.2 g, 4.26 mmol) was dissolved in MeOH (30 mL). A solution of sodium hydroxide (0.34 g, 8.5 mmol) in water (7 mL) was then added and the mixture was stirred at 70 °C for 15 min. The volatiles were then removed in vacuo, and water (20 mL) was added. The aqueous solution was allowed to return to room temperature, and the pH was adjusted to <4 by addition of a 5% aqueous citric acid solution. The precipitate was extracted with EtOAc (100 mL). The organic layer was washed with brine (30 mL) and dried ($MgSO_4$). The solvent was removed under vacuum, then Et_2O (50 mL) was added to the residue and removed in vacuo. Vacuum drying gave **48** (2.10 g, 98%) as a white foam. ^{1}H NMR (d_6-DMSO) mixture (4:5) of diastereoisomers δ 7.10 (1H, s × 2, H-9), 6.90−6.84 (1H, s × 2, H-6), 5.84−5.68 (2H, m, allyl H-2, H-11), 5.45−4.91 (3H, m, allyl H-3, pyran H-2), 4.72−4.30 (2H, m, allyl H-1), 4.09−3.93 (2H, m, side-chain H-1), 3.91−3.75 (4H, m, OCH_3), 3.60−3.44 (2H, m, H-3), 3.44−3.22 (2H, m, pyran H-6), 2.46−2.33 (2H, m, side-chain H-3), 2.20−1.76 (6H, m, side-chain H-2, H-1,2), 1.76−1.31 (6H, m, pyran H-3,4,5); MS (ES^+) *m*/*z* (relative intensity) 519 ([M + H]$^{+\bullet}$, 100%). This material was shown to be optically pure at C11a by re-esterification (EDCI, HOBt, then MeOH), THP removal (AcOH/THF/H_2O), and analysis by chiral HPLC (data not shown).

(11a*S*) Methyl 4-(7-Methoxy-5-oxo-2,3,5,11a-tetrahydro-1*H*-pyrrolo[2,1-*c*][1,4]benzodiazepine-8-yloxy)butanoate (6). A mixture of **47** (0.086 g, 162 μmol), palladium tetrakis[triphenylphosphine] (0.002 g, 1.7 μmol), and pyrrolidine (14.7 μL, 176 μmol) in anhydrous CH_2Cl_2 (10 mL) was stirred at room temperature for 1 h. The solvent was removed in vacuo and the residue purified by flash chromatography (eluted with EtOAc). The pure fractions were combined to provide **6**, (0.055 g, 98%). $[\alpha]^{26}_D = +482°$ ($c = 0.08$, $CHCl_3$); ^{1}H NMR ($CDCl_3$) δ 7.66 (1H, d, $J = 4.4$ Hz, 1H, H-11), 7.51 (1H, s, H-9), 6.80 (1H, s, H-6), 4.21−4.02 (2H, m, side-chain H-1), 3.93 (1H, s, OCH_3), 3.86−3.76 (1H, m, H-3), 3.76−3.64 (4H, m, ester OCH_3, H11a), 3.63−3.51 (1H, m, H-3), 2.54 (2H, t, J = 7.3 Hz, side-chain H-3), 2.39−2.34 (2H, m, H-1), 2.24−2.13 (2H, m, side-chain H-2), 2.12−1.95 (2H, m, H-2); MS (ES^+) *m*/*z* (relative intensity) 347 ([M + H]$^{+\bullet}$, 100%); Acc. Mass $C_{18}H_{22}N_2O_5$ calc. 347.1602 found 347.1612.

(11*S*,11a*S*)-7-Methoxy-8-[3-(5-methoxycarbonyl-1-methyl-1*H*-pyrrol-3-ylcarbamoyl)propoxy]-5-oxo-11-(tetrahydropyran-2-yloxy)-2,3,11,11a-tetrahydro-1*H*,5*H*-pyrrolo[2,1-*c*][1,4]-benzodiazepine-10-carboxylic Acid Allyl Ester (49a). A solution of pyrrole methyl ester **14** (0.055 g, 0.29 mmol) and Alloc-THP-PBD acid **48** (0.150 g, 0.29 mmol, 1 equiv) dissolved in anhydrous CH_2Cl_2 (2 mL) was treated with EDCI (0.111 g, 0.58 mmol, 2 equiv) and DMAP (0.088 g, 0.72 mmol, 2.5 equiv). After stirring for 24 h the solvent was removed in vacuo and the residue was diluted with EtOAc (25 mL) and washed with 1M HCl solution (3 × 10 mL) then saturated $NaHCO_3$ solution (3 × 10 mL). The organic fraction was dried ($MgSO_4$) and concentrated in vacuo, to give an off white foam, **49a** (0.167 g, 88%). ^{1}H NMR (d_6-acetone) mixture of diastereomers δ 9.09 (1H, s, NH), 7.39 (1H, d, $J = 2.0$ Hz, Py-H), 7.14 (1H, s, H-6), 7.12 (1H, s, H-6), 6.96 (1H, s, H-9), 6.76 (1H, d, $J = 2.0$ Hz, Py-H), 5.86−5.75 (2H, m, H-11, allyl H-2), 5.13−4.84 (3H, m, pyran H-2, allyl H-3), 4.61−4.21 (2H, m, allyl H-1), 4.06−3.88 (3H, m, side-chain H-1, pyran H-6), 3.87 (3H, s, O/NCH_3), 3.87 (3H, s, O/NCH_3), 3.86 (3H, s, O/NCH_3), 3.74 (3H, s, OCH_3), 3.53−3.44 (3H, m, H-11a, H-3), 2.55−2.45 (2H, m, side-chain H-3), 2.13−1.88 (6H, m, H-1,2, side-chain H-2), 1.70−1.39 (6H, m, pyran H-3,4,5).

(11*S*,11a*S*)-7-Methoxy-8-{3-[5-(5-methoxycarbonyl-1-methyl-1*H*-pyrrol-3-ylcarbamoyl)-1-methyl-1*H*-pyrrol-3-ylcarbamoyl]-propoxy}-5-oxo-11-(tetrahydropyran-2-yloxy)-2,3,11,11a-tetrahydro-1*H*,5*H*-pyrrolo[2,1-*c*][1,4]benzodiazepine-10-carboxylic Acid Allyl Ester (49b). The Boc-pyrrole dimer **16** (0.109 g, 0.29 mmol) was treated with 4M HCl in dioxane (2 mL). The reaction mixture was stirred at room temperature for 30 min during which time a precipitate formed. The solvent was removed and the residue dried in vacuo. The residue was dissolved in anhydrous CH_2Cl_2 (2 mL), and Alloc-THP-PBD acid **48** (0.150 g, 0.29 mmol, 1 equiv) was added followed by EDCI (0.111 g, 0.58 mmol, 2 equiv) and DMAP (0.088 g, 0.72 mmol, 2.5 equiv). After stirring for 24 h the solvent was removed in vacuo and the residue diluted with EtOAc (25 mL) and washed with 1M HCl solution (3 × 10 mL) then saturated $NaHCO_3$ solution (3 × 10 mL). The organic fraction was dried ($MgSO_4$) and concentrated in vacuo, to give a solid, (0.232 g) which was purified by column chromatography (eluted with $CHCl_3$ 97%, MeOH 3%) to give a foam, **49b** (0.115 g, 51%). ^{1}H NMR (d_6-acetone) mixture of diastereomers δ 9.20 (2H, s, NH), 7.33 (1H, d, $J = 1.8$ Hz, Py-H), 7.14 (1H, s, H-6), 7.13 (1H, s, H-6), 6.94 (1H, s, H-9), 6.92−6.90 (1H, m, Py-H), 6.90−6.89 (1H, m, Py-H), 6.81−6.80 (1H, m, Py-H), 5.86−5.75 (2H, m, H-11, allyl H-2), 5.04−4.85 (3H, s, pyran H-2, allyl H-3), 4.64−4.26 (2H, m, allyl H-1), 4.07−3.87 (4H, s, side-chain H-1, pyran H-6), 3.86 (3H, s, O/NCH_3), 3.86 (3H, s, O/NCH_3), 3.85 (3H, s, O/NCH_3), 3.77 (1H, s, OCH_3), 3.59−3.46 (3H, m, H-11a, H-3), 2.56−2.45 (2H, m, side-chain H-3), 2.15−1.92 (6H, m, H-1,2, side-chain H-2), 1.71−1.40 (6H, m, pyran H-3,4,5).

(11*S*,11a*S*)-7-Methoxy-8-(3-{5-[5-(5-methoxycarbonyl-1-methyl-1*H*-pyrrol-3-ylcarbamoyl)-1-methyl-1*H*-pyrrol-3-ylcarbamoyl]-1-methyl-1*H*-pyrrol-3-ylcarbamoyl}propoxy)-5-oxo-11-(tetrahydropyran-2-yloxy)-2,3,11,11a-tetrahydro-1*H*,5*H*-pyrrolo[2,1-*c*][1,4]benzodiazepine-10-carboxylic Acid Allyl Ester (49c). A solution of Boc-pyrrole trimer **19** (0.144 g, 0.29 mmol) was treated with 4M HCl in dioxane (2 mL). The reaction mixture was stirred at room temperature for 30 min during which time a precipitate formed. The solvent was removed and the residue dried in vacuo. The residue was dissolved in anhydrous CH_2Cl_2 (2 mL), and Alloc-THP-PBD acid **48** (0.150 g, 0.29 mmol, 1 equiv) was added followed by EDCI (0.111 g, 0.58 mmol, 2 equiv) and DMAP (0.088 g, 0.72 mmol, 2.5 equiv). After stirring for 24 h the solvent was removed in vacuo and the residue diluted with EtOAc (25 mL) and washed with 1M HCl solution (3 × 10 mL) then saturated $NaHCO_3$ solution (3 × 10 mL). The organic fraction was dried ($MgSO_4$) and concentrated in vacuo, to give an off white foam, **49c** (0.153 g, 59%). ^{1}H NMR (d_6-acetone) mixture of diastereomers δ 9.28 (1H, s, NH), 9.19 (1H, s, NH), 9.02 (1H, s, NH), 7.50 (1H, d, $J = 1.7$ Hz, Py-H), 7.23 (1H, d, $J = 1.7$ Hz, Py-H), 7.16 (1H, d, $J = 1.7$ Hz, Py-H), 7.15 (1H, s, H-6), 7.13 (1H, s, H-6), 6.99 (1H, d, $J = 1.7$ Hz, Py-H), 6.92 (1H, d, $J = 1.9$ Hz, Py-H), 6.91 (1H, s, H-9), 6.81 (1H, s, Py-H), 5.89−5.76 (2H, m, H-11, allyl H-2), 5.20−4.84 (3H, m, pyran H-2, allyl H-3), 4.61−4.25 (2H, m, allyl H-1), 4.11−3.95 (3H, m, side-chain H-1, pyran H-6), 3.94 (3H, s, O/NCH_3), 3.93 (3H, s, O/NCH_3), 3.91 (3H, s, O/NCH_3), 3.87 (3H, s, O/NCH_3), 3.76 (3H, s, OCH_3), 3.57−3.45 (3H, m, H-3, H-11a), 2.54−2.45 (2H, m, side-chain H-3), 2.12−1.88 (6H, m, H-1,2, side-chain H-2), 1.69−1.39 (6H, m, pyran H-3,4,5).

(11*S*,11a*S*)-7-Methoxy-8-[3-(5-{5-[5-(5-methoxycarbonyl-1-methyl-1*H*-pyrrol-3-ylcarbamoyl)-1-methyl-1*H*-pyrrol-3-ylcarbamoyl]-1-methyl-1*H*-pyrrol-3-ylcarbamoyl}-1-methyl-1*H*-pyrrol-3-ylcarbamoyl)propoxy]-5-oxo-11-(tetrahydropyran-2-yloxy)-2,3,11,11a-tetrahydro-1*H*,5*H*-pyrrolo[2,1-*c*][1,4]benzodiazepine-

10-carboxylic Acid Allyl Ester (49d). A solution of Boc-pyrrole tetramer **24** (0.180 g, 0.29 mmol) was treated with 4M HCl in dioxane (2 mL). The reaction mixture was stirred at room temperature for 30 min during which time a precipitate formed. The solvent was removed and the residue dried in vacuo. The residue was dissolved in anhydrous CH_2Cl_2 (2 mL), and Alloc-THP-PBD acid **48** (0.150 g, 0.29 mmol, 1 equiv) was added followed by EDCI (0.111 g, 0.58 mmol, 2 equiv) and DMAP (0.088 g, 0.72 mmol, 2.5 equiv). After stirring for 24 h the solvent was removed in vacuo and the residue diluted with EtOAc (25 mL) and washed with 1M HCl solution (3 × 10 mL) then saturated $NaHCO_3$ solution (3 × 10 mL). The organic fraction was dried ($MgSO_4$) and concentrated in vacuo, to give an off white foam, **49d** (0.068 g, 23%). ^{1}H NMR (d_6-acetone) mixture of diastereomers δ 9.28 (1H, s, NH), 9.25 (1H, s, NH), 9.18 (1H, s, NH), 9.03 (1H, s, NH), 7.50 (1H, d, J = 1.9 Hz, Py-H), 7.23 (2H, d, J = 1.4 Hz, Py-H), 7.15 (1H, s, H-6), 7.14 (1H, s, H-6), 6.99 (1H, J = 2.0 Hz, Py-H), 6.96 (1H, s, H-9), 6.93 (1H, d, J = 1.9 Hz, Py-H), 6.90 (1H, s, Py-H), 6.83 (1H, s, Py-H), 6.81 (1H, s, Py-H), 5.87−5.77 (2H, m, H-11, allyl H-2), 5.14−4.85 (3H, m, pyran H-2, allyl H-3), 4.62−4.22 (2H, m, allyl H-1), 4.09−3.95 (3H, m, side-chain H-1, pyran H-6), 3.94−3.87 (15H, 5 × s, O/NCH_3), 3.74 (3H, s, OCH_3), 3.57−3.44 (3H, m, H-3,11a), 2.49 (2H, d, J = 7.0 Hz, side-chain H-3), 2.13−1.89 (6H, m, H-1,2, side-chain H-2), 1.64−1.39 (6H, m, pyran H-3,4,5).

(11*S*,11a*S*)-7-Methoxy-8-{3-[5-(5-{5-[5-(5-methoxycarbonyl-1-methyl-1*H*-pyrrol-3-ylcarbamoyl)-1-methyl-1*H*-pyrrol-3-ylcarbamoyl]-1-methyl-1*H*-pyrrol-3-ylcarbamoyl}-1-methyl-1*H*-pyrrol-3-ylcarbamoyl)-1-methyl-1*H*-pyrrol-3-ylcarbamoyl]-propoxy}-5-oxo-11-(tetrahydropyran-2-yloxy)-2,3,11,11a-tetrahydro-1*H*,5*H*-pyrrolo[2,1-*c*][1,4]benzodiazepine-10-carboxylic Acid Allyl Ester (49e). A solution of Boc-pyrrole pentamer **26** (0.150 g, 0.20 mmol) was treated with 4M HCl in dioxane (2 mL). The reaction mixture was stirred at room temperature for 30 min during which time a precipitate formed. The solvent was removed and the residue dried in vacuo. The residue was dissolved in anhydrous CH_2Cl_2 (2 mL) and Alloc-THP-PBD acid **48** (0.150 g, 0.2 mmol, 1 equiv) was added followed by EDCI (0.111 g, 0.40 mmol, 2 equiv) and DMAP (0.088 g, 0.50 mmol, 2.5 equiv). After stirring for 24 h the solvent was removed in vacuo and the residue diluted with EtOAc (25 mL) and washed with 1M HCl solution (3 × 10 mL) then saturated $NaHCO_3$ solution (3 × 10 mL). The organic fraction was dried ($MgSO_4$) and concentrated in vacuo, to give an off white foam, **49e** (0.164 g, 71%). ^{1}H NMR (d_6-acetone) mixture of diastereomers δ 9.26−9.20 (5H, 5 × s, NH), 7.50 (1H, d, J = 1.6 Hz, Py-H), 7.23 (3H, d, J = 1.7 Hz, Py-H), 7.15 (1H, s, H-6), 6.98−6.97 (2H, m, Py-H), 6.93 (2H, d, J = 1.8 Hz, Py-H), 6.90 (1H, s, H-9), 6.84 (1H, d, J = 2.0 Hz, Py-H), 6.80 (1H, d, J = 2.0 Hz, Py-H), 5.89−5.77 (2H, m, H-11, allyl H-2), 5.14−4.86 (3H, m, pyran H-2, allyl H-3), 4.60−4.21 (2H, m, allyl H-1), 4.10−3.95 (3H, m, side-chain H-1, pyran H-6), 3.94−3.87 (18H, 6 × s, O/NCH_3), 3.76 (3H, s, OCH_3), 3.54−3.43 (3H, m, H-3,11a), 2.54−2.45 (2H, m, side-chain H-3), 2.13−1.89 (6H, m, H-1,2, side-chain H-2), 1.68−1.38 (6H, m, pyran H-3,4,5).

(11*S*,11a*S*)-7-Methoxy-8-(3-{5-[5-(5-{5-[5-(5-methoxycarbonyl-1-methyl-1*H*-pyrrol-3-ylcarbamoyl)-1-methyl-1*H*-pyrrol-3-ylcarbamoyl]-1-methyl-1*H*-pyrrol-3-ylcarbamoyl}-1-methyl-1*H*-pyrrol-3-ylcarbamoyl)-1-methyl-1*H*-pyrrol-3-ylcarbamoyl]-1-methyl-1*H*-pyrrol-3-ylcarbamoyl}propoxy)-5-oxo-11-(tetrahydropyran-2-yloxy)-2,3,11,11a-tetrahydro-1*H*,5*H*-pyrrolo[2,1-*c*]-[1,4]benzodiazepine-10-carboxylic Acid Allyl Ester (49f). A solution of Boc-pyrrole hexamer **28** (0.155 g, 0.18 mmol) was treated with 4M HCl in dioxane (2 mL). The reaction mixture was stirred at room temperature for 30 min during which time a precipitate formed. The solvent was removed and the residue dried in vacuo. The residue was dissolved in anhydrous CH_2Cl_2 (2 mL), and Alloc-THP-PBD acid **48** (0.093 g, 0.18 mmol, 1 equiv) was added followed by EDCI (0.068 g, 0.36 mmol, 2 equiv) and DMAP (0.054 g, 0.45 mmol, 2.5 equiv). After stirring for 24 h the solvent was removed in vacuo and the residue diluted with EtOAc (25 mL) and washed with 1M HCl solution (3 × 10 mL) then saturated $NaHCO_3$ solution (3 × 10 mL). The organic fraction was dried ($MgSO_4$) and concentrated in vacuo, to give an off white foam, **49f** (0.174 g, 77%). ^{1}H NMR (d_6-acetone, 500 MHz) mixture of diastereomers δ 9.28−9.16 (6H, 6 × s, NH), 7.50 (1H, d, J = 1.8 Hz, Py-H), 7.24 (3H, d, J = 1.5 Hz, Py-H), 7.16 (1H, s, H-6), 7.14 (2H, s, H-6, Py-H), 6.99 (1H, d, J = 1.7 Hz, Py-H), 6.96 (1H, s, H-9), 6.93 (4H, d, J = 1.9 Hz, Py-H), 6.83 (1H, d, J = 2.3 Hz, Py-H), 6.79 (1H, s, Py-H), 5.89−5.77 (2H, m, H-11, allyl H-2), 5.14−4.83 (3H, m, pyran H-2, allyl H-3), 4.62−4.22 (2H, m, allyl H-3), 4.12−3.95 (3H, m, side-chain H-1, pyran H-6), 3.94−3.81 (21H, 7 × s, O/NCH_3), 3.75 (3H, s, OCH_3), 3.54−3.46 (3H, m, H-3,11a), 2.54−2.46 (2H, m, side-chain H-3), 2.12−1.88 (6H, m, H-1,2, side-chain H-2), 1.68−1.38 (6H, m, pyran H-3,4,5).

(11a*S*) Methyl 4-[4-(7-Methoxy-5-oxo-2,3,5,11a-tetrahydro-5*H*-pyrrolo[2,1-*c*][1,4]benzodiazepine-8-yloxy)butyrylamino]-1-methyl-1*H*-pyrrole-2-carboxylate (50a). A solution of Alloc-THP-PBD conjugate **49a** (0.157 g, 0.24 mmol) dissolved in anhydrous CH_2Cl_2 (2 mL) under a nitrogen atmosphere was treated with pyrrolidine (22 μL, 0.26 mmol, 1.1 equiv) and then palladium tetrakis[triphenylphosphine] (0.014 g, 0.012 mmol, 0.05 equiv). The reaction mixture was stirred at room temperature for 2 h and the product purified directly by column chromatography (eluted with $CHCl_3$ 96%, MeOH 4%) to give the product as a glassy solid, **50a** (0.093 g, 83%). $[\alpha]^{27.2}{}_D$ = +351° (c = 0.08, $CHCl_3$); ^{1}H NMR (d_6-DMSO) δ 9.94 (1H, s, NH), 7.83 (1H, d, J = 4.4 Hz, H-11), 7.39 (1H, d, J = 2.0 Hz, Py-H), 7.39 (1H, s, H-6), 6.88 (1H, s, H-9), 6.76 (1H, d, J = 2.0 Hz, Py-H), 4.17−4.08 (2H, m, H-1 side-chain H-1), 3.87 (3H, s, O/NCH_3), 3.86 (3H, s, O/NCH_3), 3.77 (3H, s, OCH_3), 3.76−3.65 (2H, m, H-3,11a), 3.49−3.39 (1H, m, H-3), 2.49−2.45 (2H, m, side-chain H-3), 2.34−2.29 (2H, m, H-1), 2.13−2.05 (2H, m, side-chain H-2), 2.03−1.97 (2H, m, H-2); MS (ES^+) m/z (relative intensity) 469 ($[M + H]^{+\bullet}$, 100%) Acc. Mass $C_{24}H_{28}N_4O_6$ calc. 469.2082 found 469.2085.

(11a*S*) Methyl 4-({4-[4-(7-Methoxy-5-oxo-2,3,5,11a-tetrahydro-5*H*-pyrrolo[2,1-*c*][1,4]benzodiazepine-8-yloxy)butyrylamino]-1-methyl-1*H*-pyrrole-2-carbonyl}amino)-1-methyl-1*H*-pyrrole-2-carbxylate (50b). A solution of Alloc-THP-PBD conjugate **49b** (0.093 g, 0.12 mmol) dissolved in anhydrous CH_2Cl_2 (2 mL) under a nitrogen atmosphere was treated with pyrrolidine (11 μL, 0.13 mmol, 1.1 equiv) and then palladium tetrakis[triphenylphosphine] (0.007 g, 0.006 mmol, 0.05 equiv). The reaction mixture was stirred at room temperature for 2 h and the product purified directly by column chromatography (eluted with $CHCl_3$ 96%, MeOH 4%) to give the product as a glassy solid, **50b** (0.067 g, 95%). $[\alpha]^{27.1}{}_D$ = +348° (c = 0.022, $CHCl_3$); ^{1}H NMR (d_6-DMSO) δ 9.88 (1H, s, NH), 7.78 (1H, d, J = 4.3 Hz, H-11), 7.45 (1H, d, J = 1.7 Hz, Py-H), 7.34 (1H, s, H-6), 7.16 (1H, d, J = 1.6 Hz, Py-H), 6.90 (1H, d, J = 1.9 Hz, Py-H), 6.88 (1H, d, J = 1.8 Hz, Py-H), 6.83 (1H, s, H-9), 4.10−3.97 (2H, m, side-chain H-1), 3.84 (6H, s, O/NCH_3), 3.83 (3H, s, O/NCH_3), 3.74 (3H, s, OCH_3), 3.68−3.60 (2H, m, H-3,11a), 3.44−3.35 (1H, m, H-3), 2.45−2.42 (1H, m, side-chain H-3), 2.27−2.20 (2H, m, H-1), 2.09−1.93 (4H, m, H-2, side-chain H-2); MS (ES^+) m/z (relative intensity) 591 ($[M + H]^{+\bullet}$, 100%); Acc. Mass $C_{30}H_{34}N_6O_7$ calc. 591.2562 found 591.2535.

(11a*S*) Methyl 4-{[4-({4-[4-(7-Methoxy-5-oxo-2,3,5,11a-tetrahydro-5*H*-pyrrolo[2,1-*c*][1,4]benzodiazepine-8-yloxy)butyrylamino]-1-methyl-1*H*-pyrrole-2-carbonyl]amino)-1-methyl-1*H*-pyrrole-2-carbonyl]amino}-1-methyl-1*H*-pyrrole-2-carboxylate (50c). A solution of Alloc-THP-PBD conjugate **49c** (0.140 g, 0.16 mmol) dissolved in anhydrous CH_2Cl_2 (2 mL) under a nitrogen atmosphere was treated with pyrrolidine (15 μL, 0.17 mmol, 1.1 equiv) and then palladium tetrakis[triphenylphosphine] (0.009 g, 0.008 mmol, 0.05 equiv). The reaction mixture was stirred at room temperature for 2 h and the product purified directly by column chromatography (eluted with $CHCl_3$ 96%, MeOH 4%) to give the product as a glassy solid, **50c** (0.076 g, 68%). $[\alpha]^{27.1}{}_D$ = +185° (c = 0.077, $CHCl_3$); ^{1}H NMR (d_6-DMSO) δ 9.92 (1H, s, NH), 9.90 (1H, s, NH), 9.88 (1H, s, NH), 7.78 (1H, d, J = 4.4 Hz, H-11), 7.47 (1H, d, J = 1.9 Hz, Py-H), 7.34 (1H, s, H-6), 7.24 (1H, d, J = 1.7 Hz, Py-H), 7.17 (1H, d, J = 1.7 Hz, Py-H), 7.06 (1H, d, J = 1.8 Hz, Py-H), 6.91 (1H, d, J = 1.9 Hz, Py-H), 6.89 (1H, d, J

= 1.8 Hz, Py-H), 6.83 (1H, s, H-9), 4.14−4.05 (2H, m, side-chain H-1), 3.85 (3H, s, O/NCH_3), 3.84 (3H, s, O/NCH_3), 3.84 (3H, s, O/NCH_3), 3.83 (3H, s, O/NCH_3), 3.74 (3H, s, OCH_3), 3.67−3.61 (1H, m, H-3,11a), 3.49−3.32 (1H, m, H-3), 2.47−2.44 (2H, m, side-chain H-3), 2.30−2.23 (2H, m, H-1), 2.05−1.95 (4H, m, H-2, side-chain H-2); MS (ES^+) *m*/*z* (relative intensity) 713 ([*M* + H]$^{+\bullet}$, 100%) Acc. Mass $C_{36}H_{40}N_8O_8$ calc. 713.3042 found 713.3022.

(11a*S*) Methyl 4-[(4-{[4-({4-[4-(7-Methoxy-5-oxo-2,3,5,11a-tetrahydro-5*H*-pyrrolo[2,1-*c*][1,4]benzodiazepine-8-yloxy)butyrylamino]-1-methyl-1*H*-pyrrole-2-carbonyl]amino)-1-methyl-1*H*-pyrrole-2-carbonyl]amino}-1-methyl-1*H*-pyrrole-2-carbonyl)-amino]-1-methyl-1*H*-pyrrole-2-carboxylate (50d). A solution of Alloc-THP-PBD conjugate **49d** (0.065 g, 0.06 mmol) dissolved in anhydrous CH_2Cl_2 (2 mL) under a nitrogen atmosphere was treated with pyrrolidine (5 μL, 0.07 mmol, 1.1 equiv) and then palladium tetrakis[triphenylphosphine] (0.004 g, 0.003 mmol, 0.05 equiv). The reaction mixture was stirred at room temperature for 2 h and the product purified directly by column chromatography (eluted with $CHCl_3$ 96%, MeOH 4%) to give the product as a glassy solid, **50d** (0.029 g, 55%). $[\alpha]^{26.5}_D$ = +129° (*c* = 0.031, $CHCl_3$); ^{1}H NMR (d_6-DMSO) δ 9.94 (1H, s, NH), 9.93 (1H, s, NH), 9.90 (1H, s, NH), 9.88 (1H, s, NH), 7.78 (1H, d, *J* = 4.4 Hz, H-11), 7.48 (1H, d, *J* = 1.3 Hz, Py-H), 7.35 (1H, s, H-6), 7.25 (2H, s, Py-H), 7.17 (1H, d, *J* = 0.8 Hz, Py-H), 7.08 (1H, d, *J* = 1.1 Hz, Py-H), 7.06 (1H, d, *J* = 0.9 Hz, Py-H), 6.92 (1H, d, *J* = 1.2 Hz, Py-H), 6.90 (1H, s, Py-H), 6.83 (1H, s, H-9), 4.14−4.05 (2H, m, side-chain H-1), 3.86−3.83 (15H, 5 × s, O/NCH_3), 3.75 (3H, s, OCH_3), 3.68−3.61 (2H, m, H-3,11a), 3.46−3.30 (1H, m, H-3), 2.47−2.43 (2H, m, side-chain H-3), 2.26−2.18 (2H, m, H-1), 2.05−1.94 (4H, m, H-2, side-chain H-2); MS (ES^+) *m*/*z* (relative intensity) 835 ([*M* + H]$^{+\bullet}$, 100%); Acc. Mass $C_{42}H_{46}N_{10}O_9$ calc. 835.3522 found 835.3497.

(11a*S*) Methyl 4-({4-[(4-{[4-({4-[4-(7-Methoxy-5-oxo-2,3,5,-11a-tetrahydro-5*H*-pyrrolo[2,1-*c*][1,4]benzodiazepine-8-yloxy)-butyrylamino]-1-methyl-1*H*-pyrrole-2-carbonyl]amino)-1-methyl-1*H*-pyrrole-2-carbonyl]amino}-1-methyl-1*H*-pyrrole-2-carbonyl)amino]-1-methyl-1*H*-pyrrole-2-carbonyl}amino)-1-methyl-1*H*-pyrrole-2-carboxylate (50e). A solution of Alloc-THP-PBD conjugate **49e** (0.164 g, 0.14 mmol) dissolved in anhydrous CH_2Cl_2 (2 mL) under a nitrogen atmosphere was treated with pyrrolidine (13 μL, 0.16 mmol, 1.1 equiv) and then palladium tetrakis[triphenylphosphine] (0.008 g, 0.007 mmol, 0.05 equiv). The reaction mixture was stirred at room temperature for 2 h and the product purified directly by column chromatography (eluted with $CHCl_3$ 96%, MeOH 4%) to give the product as a glassy solid, **50e** (0.068 g, 50%). $[\alpha]^{26.7}_D$ = +90° (*c* = 0.068, $CHCl_3$); ^{1}H NMR (d_6-DMSO) δ 9.95 (1H, s, NH), 9.95 (1H, s, NH), 9.94 (1H, s, NH), 9.91 (1H, s, NH), 9.89 (1H, s, NH), 7.78 (1H, d, *J* = 4.4 Hz, H-11), 7.48 (1H, d, *J* = 1.8 Hz, Py-H), 7.35 (1H, s, H-6), 7.25 (3H, s, Py-H), 7.17 (1H, d, *J* = 1.6 Hz, Py-H), 7.09 (1H, d, *J* = 2.1 Hz, Py-H), 7.08 (1H, s, Py-H), 7.07 (1H, d, *J* = 1.6 Hz, Py-H), 6.92 (1H, d, *J* = 1.9 Hz, Py-H), 6.91 (1H, d, *J* = 1.8 Hz, Py-H), 6.83 (1H, s, H-9), 4.14−4.05 (2H, m, side-chain H-1), 3.87−3.83 (18H, 6 × s, O/NCH_3), 3.75 (3H, s, OCH_3), 3.68−3.60 (2H, m, H-3,11a), 3.47−3.31 (1H, m, H-3), 2.47−2.44 (2H, m, side-chain H-3), 2.30−2.23 (2H, m, H-1), 2.06−1.94 (4H, m, H-2, side-chain H-2); MS (ES^+) *m*/*z* (relative intensity) 957 ([*M* + H]$^{+\bullet}$, 90%); Acc. Mass $C_{48}H_{52}N_{12}O_{10}$ calc. 957.4002 found 957.4010.

(11a*S*) Methyl 4-{[4-({4-[(4-{[4-({4-[4-(7-Methoxy-5-oxo-2,3,5,11a-tetrahydro-5*H*-pyrrolo[2,1-*c*][1,4]benzodiazepine-8-yloxy)butyrylamino]-1-methyl-1*H*-pyrrole-2-carbonyl]amino)-1-methyl-1*H*-pyrrole-2-carbonyl]amino}-1-methyl-1*H*-pyrrole-2-carbonyl)amino]-1-methyl-1*H*-pyrrole-2-carbonyl}amino)-1-methyl-1*H*-pyrrole-2-carbonyl]amino}-1-methyl-1*H*-pyrrole-2-carboxylate (50f). A solution of Alloc-THP-PBD conjugate **49f** (0.174 g, 0.14 mmol) dissolved in anhydrous CH_2Cl_2 (2 mL) under a nitrogen atmosphere was treated with pyrrolidine (13 μL, 0.15 mmol, 1.1 equiv) and then palladium tetrakis[triphenylphosphine] (0.008 g, 0.007 mmol, 0.05 equiv). The reaction mixture was stirred at room temperature for 2 h and the product purified directly by column chromatography (eluted with $CHCl_3$ 96%, MeOH 4%) to give the product as a glassy solid, **50f** (0.084 g, 57%). $[\alpha]^{27.1}_D$ = +107° (*c* = 0.084, $CHCl_3$); ^{1}H NMR (d_6-DMSO) δ 9.96 (2H, s, NH), 9.95 (1H, s, NH), 9.94 (1H, s, NH), 9.91 (1H, s, NH), 9.89 (1H, s, NH), 7.78 (1H, d, *J* = 4.4 Hz, H-11), 7.35 (1H, s, H-6), 7.27−7.25 (4H, m, Py-H), 7.17 (1H, d, *J* = 1.6 Hz, Py-H), 7.09 (2H, d, *J* = 1.5 Hz, Py-H), 7.08 (2H, d, *J* = 1.7 Hz, Py-H), 6.92 (1H, d, *J* = 1.9 Hz, Py-H), 6.91 (1H, d, *J* = 1.8 Hz, Py-H), 6.84 (1H, s, H-9), 4.14−4.05 (2H, m, side-chain H-1), 3.87−3.83 (21H, 7 × s, O/NCH_3), 3.75 (3H, s, OCH_3), 3.68−3.61 (2H, m, H-3,-11a), 3.48−3.32 (1H, m, H-3), 2.46−2.43 (2H, m, side-chain H-3), 2.29−2.23 (2H, m, H-1), 2.06−1.94 (4H, m, H-2, side-chain H-2); MS (ES^+) *m*/*z* (relative intensity) 1079 ([*M* + H]$^{+\bullet}$, 50%); Acc. mass $C_{54}H_{58}N_{14}O_{11}$ calc. 1079.4482 found 1079.4542.

(11a*S*)-4-(7-Methoxy-5,11-dioxo-2,3,4,10,11a-hexahydro-1*H*-pyrrolo[2,1-*c*][1,4]benzodiazepine-8-yloxy)butanoic acid (55). The benzyl ester **54** (3.58 g, 8.17 mmol) was dissolved in EtOH (40 mL), and a suspension of 10% palladium on charcoal (0.358 g) in EtOAc (5 mL) was added. The reaction mixture was agitated under a hydrogen atmosphere (50 psi) for 2.5 h then filtered through a Celite pad. The Celite was washed with EtOAc then the combined filtrates were concentrated in vacuo, then dried in vacuo to give the product as a white foam **55** (2.44 g, 100%). ^{1}H NMR (d_6-DMSO) δ 11.96 (1H, s, COOH), 10.21 (1H, s, NH), 7.23 (1H, s, H-6), 6.68 (1H, s, H-9), 4.06 (2H, d, *J* = 7.3 Hz, side-chain H-1), 4.03−3.94 (2H, m, H-11a), 3.78 (3H, s, OCH_3), 3.58−3.52 (1H, m, H-3), 3.48−3.42 (1H, m, H-3), 2.49−2.44 (1H, m, H-1), 2.39 (2H, t, *J* = 7.2 Hz, side-chain H-3), 1.96 (2H, p, *J* = 7.2 Hz, side-chain H-2), 1.94−1.76 (3H, m, H-1,2).

4-{[4-({4-[4-((11a*S*)-7-methoxy-1,2,3,10,11,11a-hexahydro-5*H*-pyrrolo[2,1-c][1,4]benzodiazepine-5,11-dione)-8-yloxy)butyryl-amino]-1-methyl-1*H*-pyrrole-2-carbonyl}amino)-1-methyl-1*H*-pyrrole-2-carbonyl]-amino}-1-methyl-1*H*-pyrrole-2-carboxylic Acid Methyl Ester (56). A solution of Boc pyrrole trimer **19** (0.200 g, 0.40 mmol) was treated with 4M HCl in dioxane (2 mL). The reaction mixture was stirred at room temperature for 30 min during which time a precipitate formed. The solvent was removed and the residue dried in vacuo. The residue was dissolved in anhydrous CH_2Cl_2, and **55** (0.140 g, 0.4 mmol, 1 equiv) was added followed by EDCI (0.115 g, 0.6 mmol, 1.5 equiv) and DMAP (0.059 g, 0.48 mmol, 1.2 equiv). The reaction mixture was stirred for 24 h then the solvent was removed in vacuo and the residue diluted with EtOAc (25 mL) and washed with 1M HCl solution (3 × 10 mL) then saturated $NaHCO_3$ solution (3 × 10 mL). The organic fraction was dried ($MgSO_4$) and concentrated in vacuo, to give a solid, which was purified by column chromatography (eluted with EtOAc−hexane 30:70−75:25) and by preparative LC-MS (Phenomenex Luna-Combi-HTS 5 × 100 mm × 21.2 mm column, flow rate 32 mL/min and a gradient solvent system going from 90:10 solvent A:B at time 0−1.35 min to 10:90 A:B at 5.85 min after sample injection then maintained at 10:90 until 6.85 min. Solvent A − 0.1% formic acid in water, solvent B − 0.1% formic acid in acetonitrile) and lyophilized to afford a white solid **56**, (0.016 g, 6%) as a racemic mixture. ^{1}H NMR (d_6-DMSO) δ 10.20 (1H, s, NH), 9.92 (1H, s, NH), 9.90 (1H, s, NH), 9.88 (1H, s, NH), 7.46 (1H, d, *J* = 2.0 Hz, Py-H), 7.25 (1H, s, H-6), 7.23 (1H, d, *J* = 1.6 Hz, Py-H), 7.17 (1H, d, *J* = 2.0 Hz, Py-H), 7.05 (1H, d, *J* = 1.6 Hz, Py-H), 6.90 (1H, d, *J* = 2.0 Hz, Py-H), 6.87 (1H, d, *J* = 1.6 Hz, Py-H), 6.69 (1H, s, H-9), 4.06−4.03 (2H, m, side-chain H-1), 4.01−3.97 (2H, m, side-chain H-3), 3.84 (3H, s, NCH_3), 3.84 (3H, s, NCH_3), 3.83 (3H, s, NCH_3), 3.79 (3H, s, OCH_3), 3.74 (3H, s, OCH_3), 3.71−3.64 (1H, m, H-11a), 3.57−3.51 (2H, m, H-3), 3.47−3.41 (2H, m, H-4), 2.09−2.02 (2H, m, side-chain H-2), 1.94−1.87 (2H, m, H-2); Acc. Mass $C_{36}H_{40}N_8O_9$ calc. 729.2991 found 729.2988.

Thermal Denaturation Studies. The PBD agents were subjected to DNA thermal melting (denaturation) studies[33,39,49] using duplex-form calf thymus DNA (CT-DNA, type-I, highly polymerized sodium salt; 42% G+C [Sigma]) at a fixed 100 μM (DNAp equivalent to 50 μM in bp) concentration, determined using an extinction coefficient of 6600 (M phosphate)$^{-1}$ cm^{-1} at 260 nm.[50] Solutions were prepared in pH 7.00 ± 0.01 aqueous buffer

containing 10 mM NaH_2PO_4/Na_2HPO_4 and 1 mM EDTA. Working solutions containing CT-DNA and the test compound (5 μM) were incubated at 37.0 ± 0.1 °C at 0, 4, or 18 h intervals using an external water bath. Samples were monitored at 260 nm using a Varian-Cary 4000 spectrophotometer fitted with a Peltier heating accessory. Heating was applied at a rate of 1 °C/min in the 45−98 °C temperature range, following equilibration of samples at 45 °C for 15 min, with optical and temperature data sampling at 100 ms intervals. A separate experiment was carried out using buffer alone, and this baseline was subtracted from each DNA melting curve before data treatment. Optical data were imported into the Origin 5 program (MicroCal Inc., Northampton, MA) for analysis. DNA helix→coil transition temperatures (T_m) were determined at the midpoint of the normalized melting profiles using a published analytical procedure.[39] Results are given as the mean ± standard deviation from at least three determinations. Ligand-induced alterations in DNA melting behavior (ΔT_m) are given by $\Delta T_m = T_m$(DNA + ligand) − T_m(DNA), where the T_m value determined for free CT-DNA is 67.82 ± 0.06 °C (averaged from >100 runs). All assay compounds were dissolved in HPLC-grade DMSO to give working solutions containing ≤0.2% v/v DMSO; T_m results were corrected for the effects of DMSO cosolvent by using a linear correction term. Other [DNAp]/[ligand] molar ratios (i.e., 20:1, 5:1 and 2:1) were examined to ensure that the fixed 10:1 ratio used in this assay did not result in saturation of the host CT-DNA duplex.

DNA Footprinting. Forward (5′-CAGGAAACAGCTATGAC-3′) or reverse (5′-GTAAAACGACGGCCAGT-3′) primer was 5′-end labeled with ^{32}P by T4 polynucleotide kinase. Labeling mixture contained primer (5 pmol; Sigma-Genosys), 10x kinase buffer (1 μL; Promega), (γ-^{32}P)-ATP (2 μL of 10 μCi/μL, 6000 Ci/mmol; Perkin-Elmer Life Sciences) and T4 polynucleotide kinase (10 U; Promega) in a 10 μL final volume. This mixture was incubated at 37 °C for 30 min followed by inactivation of the kinase at 70 °C for 10 min. A 262-bp DNA fragment (MS2F or MS2R) was amplified from the MS2 plasmid using PCR with either labeled forward or reverse primer and the unlabeled primer as required. Reactions were comprised of labeled primer mix (10 μL), 10x PCR buffer (5 μL; Sigma), dNTPs (5 μL; 2.5 mM each of A, C, G and T, Amersham Pharmacia), unlabeled primer as required (5 pmol), MS2 plasmid template DNA (10 ng) and Taq DNA polymerase (5 U; Sigma) in a 50 μL final volume. Radiolabeled 262-mer was purified by nondenaturing polyacrylamide gel electrophoresis, elution, filtration, and EtOH precipitation, and was then resuspended in a solution of Tris-HCl (10 mM) pH 7.4/NaCl (10 mM) to yield an activity of 200 counts per second per 5 μL when held up, in a pipet tip, to a capped Morgan series 900 mini-monitor.

For DNase I footprinting, radiolabeled 262-mer (2 μL) was incubated overnight (16−18 h) with either drug solution (388 μL) or an aqueous buffer [HEPES (20 mM) pH 7.9, NaCl (50 mM), $MgCl_2$ (1 mM), DTT (5 mM), 10% glycerol] for control reactions. Enzymatic cleavage was initiated by addition of DNase I solution (10 μL of 0.05 U/mL; Sigma) in aqueous NaCl (200 mM), $MgCl_2$ (20 mM) and $MnCl_2$ (20 mM), and halted with stop solution [40 μL of NaCl (2.25 M), EDTA (150 mM) pH 8.0, 0.57 μg/μL glycogen (0.57 μg/μL; Roche), poly(dI-dC)·poly(dI-dC) DNA (19.3 ng/μL; Amersham Pharmacia)]. From this mixture, digested DNA fragments were prepared for electrophoresis following the protocol of Trauger & Dervan[51] and were loaded on to a preheated 8% denaturing polyacrylamide gel. Electrophoresis in 1x TBE buffer was allowed to proceed for 100 min at 70 W (1600−2000 V). The gel was then fixed in acetic acid (10% v/v) and CH_3OH (10% v/v) for 15 min followed by blotting onto Whatman 3MM paper and vacuum-drying at 80 °C for 45 min.

Dried gels were stored at room temperature in phosphor storage screens (Molecular Dynamics) for a minimum period of 12 h. Data were collected from exposed screens using a Molecular Dynamics 425E PhosphorImager and transferred to ImageQuant v1.2 software (Molecular Dynamics) for analysis. Data were expressed as the differential cleavage between control and sample lanes. Peaks were integrated and differential cleavage calculated as $\ln(f_d) - \ln(f_c)$, where f_d is the fractional cleavage at any particular bond in the presence of drug and f_c is the fractional cleavage of the same bond in the control. Maxam−Gilbert G + A marker lanes were prepared in the usual fashion.

In Vitro Transcription. An extended 282-bp DNA fragment, containing the 262-bp sequence used in the footprinting assays and a suitably positioned 5′ T7 promoter, was amplified from the MS2 plasmid by PCR with MS2-T7 forward primer (5′-TAATAC-GACTCACTATAGGGCAGGAAACAGCTATGAC-3′) and reverse primer (see DNA Footprinting section above). The 282-mer product was purified by phenol−$CHCl_3$ extraction and EtOH precipitation before being resuspended in nuclease-free water to a fixed concentration (1 μg/μL).

The 282-mer (1 μL) was incubated overnight with either 1.25x drug solution (4 μL) or water as a control. Transcription mix [5 μL total containing 5x transcription buffer (2 μL), RNasin RNase inhibitor (0.5 μL of 40 U/μL), T7 RNA polymerase (0.25 μL of 20 U/μL), DTT (0.25 μL, 100 mM; all Promega), NTPs (0.5 μL of 25 mM A, C, G and T, Amersham Pharmacia), (α-^{32}P)-CTP (0.25 μL of 10 μCi/μL, 3000 Ci/mmol, Perkin-Elmer Life Sciences) and nuclease-free water (1.25 μL)] was added, and synthesis of RNA transcripts was allowed to proceed at 37 °C for 90 min. Following the addition of loading dye (10 μL), samples were heated to 94 °C for 4 min, briefly cooled on ice, and then loaded on to a preheated 8% denaturing polyacrylamide gel. Electrophoresis was performed for 80 min in 0.5x TBE buffer at 60 W (2000−2250 V). The gel was then blotted onto Whatman 3MM paper and dried under vacuum at 80 °C for 45 min. Exposure to phosphor storage screens and data collection were carried out as for the footprinting gels.

Marker lanes were created by restriction enzyme digestion of the 282-mer. Ten different restriction enzymes, each with a single cutting site on the 282-mer, were employed to cleave the template 282-mer DNA in separate reactions according to the manufacturer's guidelines. Cut DNA was pooled and purified by phenol−$CHCl_3$ extraction and EtOH precipitation. The DNA was resuspended in nuclease-free water to give a fixed concentration (1 μg/μL). Marker DNA (1 μL) was used as a template for transcription as described above, yielding RNA transcripts of known length depending on the enzyme cutting site. Therefore, the marker lengths differ for particular experiments depending upon the enzymes chosen.

The lengths of attenuated transcripts produced in the presence of drug were calculated by a graphical method. The electrophoresed distance was accurately measured for each marker band, and a plot of the length of the transcript against this distance was curve-fitted. The electrophoresed distance of each attenuated transcript was then used to determine its approximate length and hence the position of the transcription stop site on the DNA template.

Determination of In Vitro Cytotoxicity. K562 human chronic myeloid leukemia cells were maintained in RPMI 1640 medium supplemented with 10% fetal calf serum and glutamine (2 mM) at 37 °C in a humidified atmosphere containing 5% CO_2. Cells were plated at 1×10^4 cells per well in media (190 μL) in 96-well plates. Compounds were serially diluted in 0.6% DMSO and added to the cell plates in triplicate (10 μL per well). Control wells containing vehicle control of 0.6% DMSO were included, and outer columns were used as blanks. Plates were kept in the dark at 37 °C in a humidified atmosphere containing 5% CO_2. Following a 4-day incubation (to allow control cells to increase in number by approximately 10-fold), the MTT assay was used to determine cell viability. This assay is based on the ability of viable cells to reduce a yellow soluble tetrazolium salt, 3-(4,5-dimethylthiazol-2-yl)-2,5-diphenyl-2*H*-tetrazolium bromide (MTT, Sigma-Aldrich), to an insoluble purple formazan precipitate. MTT solution (25 μL of 5 mg/mL in phosphate-buffered saline) was added to each well and the plates further incubated for 4 h. The bulk of the medium was then pipetted from the cell pellet. DMSO (200 μL) was added to each well in order to solubilize the purple formazan dye. The optical density was then read at 540 nm on a Fusion plate reader (Perkin-Elmer). A dose−response curve was constructed using GraphPad Prism 4.01 (GraphPad Software Inc.) from $n = 2$ data (from two individual experiments). An IC_{50} value was read as the

dose required to reduce the final optical density to 50% of the control value.

Cellular and Nuclear Penetration into MCF-7 Human Mammary Cells. Cellular uptake and nuclear incorporation of drug into MCF-7 human mammary adenocarcinoma cells (ATCC Collection, LGC Promochem) was visualized using confocal microscopy. Solutions of conjugates **50a**−**f** were prepared in DMSO at 20 mM and diluted in Hank's Balanced Salt Solution (Sigma) to the appropriate concentration. Freshly harvested MCF7 cells at 5×10^4 cells/mL were placed in 200 μL of complete RPMI1640 (containing 10% FCS) contained in the wells of eight-well chambered cover-glasses. The cells were incubated overnight to adhere at 37 °C. Cellular preparations were then spiked with the conjugates to give final concentrations of 1, 10, and 100 μM, ensuring that final DMSO concentrations were <1% v/v. At 1, 3, 5, and 24 h after addition of the conjugates, the cells were examined using a Zeiss LSM510 inverted microscope with UV laser excitation. Samples were viewed under oil immersion with a 60× objective lens. Representative images for conjugates **50a**, **50c**, and **50f** are shown in Figure 8.

Acknowledgment. This work was supported by Cancer Research UK (C180/A1060, SP1938/0402, SP1938/0201 and SP1938/0301 to D.E.T., J.A.H., and T.C.J., C459/A2579 to S.D.S. and P.M.L.) and by Spirogen Ltd. Z.A.S. was supported by studentship 00A1E06372 from the BBSRC. Dr. Robert Schultz of the National Cancer Institute (NCI) is thanked for providing the 60-cell line data shown in Table 1. Dr. Fatima A. Delmani is acknowledged for providing preliminary cytotoxicity data not appearing in this paper, as is Dr. Tom Ellis for his contribution to the development of the gel-based assays. The EPSRC is thanked for funding an NMR upgrade (GR/R47646/01) in the School of Pharmacy.

Supporting Information Available: S1-A: Footprinting Gels for **50a** and **50b** (Forward-labeled MS2F DNA fragment); S1-B: Footprinting Gel for **50d** (Forward-labeled MS2F DNA fragment); S1-C: Footprinting Gels for **50d** (Forward- and Reverse-labeled MS2 DNA fragments); S1-D: Footprinting Gel for **50f** (Forward-labeled MS2F DNA Fragment); S2-A: Analysis of footprints from the MS2F DNA (Forward-labeled DNA fragment); S2-B: Analysis of footprints from the MS2R DNA (Reverse-labeled DNA fragment); S3: Differential cleavage plots showing the relative positions of footprints produced by **50c**, **23,** and **3** (anthramycin methyl ether); S4: DNase I footprinting gels of **3** binding to both MS2F (Forward-labeled) and MS2R (Reverse-labeled) DNA fragments; S5: DNase I footprinting gels of compound **38** binding to both MS2F (Forward-labeled) and MS2R (Reverse-labeled) DNA fragments; S6: Comparative differential cleavage plots for compounds **50c** and **38**; S7-A: In vitro transcription gel showing the T-stops produced by **50a** on the MS2 DNA fragment; S7-B: In vitro transcription gel showing the T-stops produced by **50b** on the MS2 DNA fragment; S7-C**:** In vitro transcription gel showing the T-stops produced by **50d** on the MS2 DNA fragment; S7-D: In vitro transcription gel showing the T-stops produced by **50e** on the MS2 DNA fragment; S7-E: In vitro transcription gel showing the T-stops produced by **50f** on the MS2 DNA fragment; **S8**: In vitro transcription gel showing the T-stops produced by **3** on the MS2 DNA fragment; S9: Experimental details (and references) for synthesis of compounds **16**, **17**, **19**, **20**, **24**, **26**, **28**, **31**, **32**, **40**−**45**, and **52**−**54**; S10: ^{13}C NMR and IR data for compounds **6**, **22**, **35**, **38**, **46**−**48**, **50a**−**f**; S11: HPLC data for key compounds **6**, **22**, **38**, **50a**−**f**, and **56**. This material is available free of charge via the Internet at http://pubs.acs.org.

References

(1) Dervan, P. B.; Edelson, B. S., Recognition of the DNA Minor Groove by Pyrrole-Imidazole Polyamides. *Curr. Opin. Struct. Biol.* **2003**, *13* (3), 284−299.

(2) Best, T. P.; Edelson, B. S.; Nickols, N. G.; Dervan, P. B., Nuclear Localization of Pyrrole-Imidazole Polyamide-Fluorescein Conjugates in Cell Culture. *Proc. Natl. Acad. Sci. U.S.A.* **2003**, *100* (21), 12063−12068.

(3) Dudouet, B.; Burnett, R.; Dickinson, L. A.; Wood, M. R.; Melander, C.; Belitsky, J. M.; Edelson, B.; Wurtz, N.; Briehn, C.; Dervan, P. B.; Gottesfeld, J. M. Accessibility of nuclear chromatin by DNA binding polyamides. *Chem. Biol.* **2003**, *10* (9), 859−67.

(4) Thurston, D. E. Nucleic Acid Targeting: Therapeutic Strategies for the 21st Century. *Br. J. Cancer* **1999**, *80* (S1), 65−85.

(5) Thurston, D. E. Advances in the Study of Pyrrolo[2,1-*c*][1,4]-benzodiazepine (PBD) Antitumour Antibiotics. In *Molecular Aspects of Anticancer Drug*−*DNA Interactions*; Neidle, S., Waring, M. J., Eds.; The Macmillan Press Ltd., London, UK: London, 1993; Vol. 1, pp 54−88.

(6) Kamal, A.; Babu, A. H.; Ramana, A. V.; Ramana, K. V.; Bharathi, E. V.; Kumar, M. S. Synthesis of Pyrrolo[2,1-*c*][1,4]benzodiazepines and Their Conjugates by Azido Reductive Cyclization Strategy as Potential DNA-Binding Agents. *Bioorg. Med. Chem. Lett.* **2005**, *15* (10), 2621−2623.

(7) Kamal, A.; Reddy, D. R.; Reddy, P.; Rajendar, Synthesis and DNA-Binding Ability of Pyrrolo[2,1-*c*][1,4]benzodiazepine-Azepane Conjugates. *Bioorg. Med. Chem. Lett.* **2006**, *16* (5), 1160−1163.

(8) Wang, J. J.; Shen, Y. K.; Hu, W. P.; Hsieh, M. C.; Lin, F. L.; Hsu, M. K.; Hsu, M. H., Design, Synthesis, and Biological Evaluation of Pyrrolo[2,1-*c*][1,4]benzodiazepine and Indole Conjugates as Anticancer agents. *J. Med. Chem.* **2006**, *49* (4), 1442−1449.

(9) Damayanthi, Y.; Reddy, B. S. P.; Lown, J. W. Design and Synthesis of Novel Pyrrolo[2,1-*c*][1,4]benzodiazepine-Lexitropsin Conjugates. *J. Org. Chem.* **1999**, *64* (1), 290−292.

(10) Reddy, B. S. P.; Damayanthi, Y.; Reddy, B. S. N.; Lown, J. W. Design, Synthesis and In Vitro Cytotoxicity Studies of Novel Pyrrolo-[2,1-*c*][1,4]benzodiazepine (PBD)-Polyamide Conjugates and 2,2′-PBD Dimers. *Anti-Cancer Drug Des.* **2000**, *15* (3), 225−238.

(11) Kumar, R.; Lown, J. W. Synthesis and Antitumor Cytotoxicity Evaluation of Novel Pyrrolo[2,1-*c*][1,4]benzodiazepine Imidazole Containing Polyamide Conjugates. *Oncol. Res.* **2003**, *13* (4), 221−233.

(12) Kumar, R.; Reddy, B. S. N.; Lown, J. W. Design and Synthesis of Novel Pyrrolo[2,1-*c*][1,4]benzodiazepine-Imidazole Containing Polyamide Conjugates. *Heterocycl. Commun.* **2002**, *8* (1), 19−26.

(13) Baraldi, P. G.; Cacciari, B.; Guiotto, A.; Leoni, A.; Romagnoli, R.; Spalluto, G.; Mongelli, N.; Howard, P. W.; Thurston, D. E.; Bianchi, N.; Gambari, R. Design, Synthesis and Biological Activity of a Pyrrolo[2,1-*c*][1,4]benzodiazepine (PBD)-Distamycin Hybrid. *Bioorg. Med. Chem. Lett.* **1998**, *8* (21), 3019−3024.

(14) Kumar, R.; Lown, J. W. Design, Synthesis and In Vitro Cytotoxicity Studies of Novel Pyrrolo[2,1][1,4]benzodiazepine-Glycosylated Pyrrole and Imidazole Polyamide Conjugates. *Org. Biomol. Chem.* **2003**, *1* (19), 3327−3342.

(15) Baraldi, P. G.; Balboni, G.; Cacciari, B.; Guiotto, A.; Manfredini, S.; Romagnoli, R.; Spalluto, G.; Thurston, D. E.; Howard, P. W.; Bianchi, N.; Rutigliano, C.; Mischiati, C.; Gambari, R. Synthesis, In Vitro Antiproliferative Activity, and DNA-Binding Properties of Hybrid Molecules Containing Pyrrolo[2,1-*c*][1,4]benzodiazepine and Minor-Groove-Binding Oligopyrrole Carriers. *J. Med. Chem.* **1999**, *42* (25), 5131−5141.

(16) Borgatti, M.; Rutigliano, C.; Bianchi, N.; Mischiati, C.; Baraldi, P. G.; Romagnoli, R.; Gambari, R. Inhibition of NF-kB/DNA Interactions and HIV-1 LTR Directed Transcription by Hybrid Molecules Containing Pyrrolo[2,1-*c*][1,4]benzodiazepine (PBD) and Oligopyrrole Carriers. *Drug Dev. Res.* **2003**, *60* (3), 173−185.

(17) Baraldi, P. G.; Cacciari, B.; Guiotto, A.; Romagnoli, R.; Spalluto, G.; Leoni, A.; Bianchi, N.; Feriotto, G.; Rutigliano, C.; Mischiati, C.; Gambari, R. [2,1-c][1,4]Benzodiazepine (PBD)-Distamycin Hybrid Inhibits DNA Binding to Transcription Factor Sp1. *Nucleosides Nucleotides Nucleic Acids* **2000**, *19* (8), 1219−1229.

(18) Mischiati, C.; Finotti, A.; Sereni, A.; Boschetti, S.; Baraldi, P. G.; Romagnoli, R.; Feriotto, G.; Jeang, K. T.; Bianchi, N.; Borgatti, M.; Gambari, R. Binding of Hybrid Molecules Containing Pyrrolo[2,1-*c*][1,4]benzodiazepine (PBD) and Oligopyrrole Carriers to the Human Immunodeficiency Type 1 Virus TAR−RNA. *Biochem. Pharmacol.* **2004**, *67* (3), 401−410.

(19) Kollman, P. A.; Massova, I.; Reyes, C.; Kuhn, B.; Huo, S. H.; Chong, L.; Lee, M.; Lee, T.; Duan, Y.; Wang, W.; Donini, O.; Cieplak, P.; Srinivasan, J.; Case, D. A.; Cheatham, T. E. Calculating Structures and Free Energies of Complex Molecules: Combining Molecular Mechanics and Continuum Models. *Acc. Chem. Res.* **2000**, *33* (12), 889−897.

(20) Swalley, S. E.; Baird, E. E.; Dervan, P. B. Recognition of a 5′-(A,T)-GGG(A,T)(2)-3′ sequence in the minor groove of DNA by an eight-ring hairpin polyamide. *J. Am. Chem. Soc.* **1996**, *118* (35), 8198−8206.

(21) Boger, D. L.; Fink, B. E.; Hedrick, M. P. Total Synthesis of Distamycin A and 2640 Analogues: A Solution-Phase Combinatorial Approach to the Discovery of New, Bioactive DNA Binding Agents and Development of a Rapid, High-Throughput Screen for Determining Relative DNA Binding Affinity or DNA Binding Sequence Selectivity. *J. Am. Chem. Soc.* **2000**, *122* (27), 6382−6394.
(22) Bhattacharya, S.; Thomas, M. Facile Synthesis of Oligopeptide Distamycin Analogues Devoid of Hydrogen Bond Donors or Acceptors at the N−Terminus: Sequence-Specific Duplex DNA Binding as a Function of Peptide Chain Length. *Tetrahedron Lett.* **2000**, *41* (29), 5571−5575.
(23) Mrani, D.; Gosselin, G.; Auclair, C.; Balzarini, J.; Declercq, E.; Paoletti, C.; Imbach, J. L. Synthesis, DNA-Binding and Biological-Activity of Oxazolopyridocarbazole-Netropsin Hybrid Molecules. *Eur. J. Med. Chem.* **1991**, *26* (5), 481−488.
(24) Yeung, B. K. S.; Boger, D. L. Synthesis of Isochrysohermidin-Distamycin Hybrids. *J. Org. Chem.* **2003**, *68* (13), 5249−5253.
(25) Fukuyama, T.; Liu, G.; Linton, S. D.; Lin, S. C.; Nishino, H. Total Synthesis of (+)-Porothramycin-B. *Tetrahedron Lett.* **1993**, *34* (16), 2577−2580.
(26) Thurston, D. E.; Bose, D. S.; Howard, P. W.; Jenkins, T. C.; Leoni, A.; Baraldi, P. G.; Guiotto, A.; Cacciari, B.; Kelland, L. R.; Foloppe, M. P.; Rault, S. Effect of A-Ring Modifications on the DNA-Binding Behavior and Cytotoxicity of Pyrrolo[2,1-*c*][1,4]benzodiazepines. *J. Med. Chem.* **1999**, *42* (11), 1951−1964.
(27) Masterson, L. A.; Croker, S. J.; Jenkins, T. C.; Howard, P. W.; Thurston, D. E. Synthesis and Biological Evaluation of Pyrrolo[2,1-*c*][1,4]benzodiazepine (PBD) C8 Cyclic Amine Conjugates. *Bioorg. Med. Chem. Lett.* **2004**, *14* (4), 901−904.
(28) McMinn, D. L.; Greenberg, M. M. Novel Solid-Phase Synthesis Supports for the Preparation of Oligonucleotides Containing S3′-Alkylamines. *Tetrahedron* **1996**, *52* (11), 3827−3840.
(29) Tercel, M.; Stribbling, S. M.; Sheppard, H.; Siim, B. G.; Wu, K.; Pullen, S. M.; Botting, K. J.; Wilson, W. R.; Denny, W. A. Unsymmetrical DNA Cross-Linking Agents: Combination of the CBI and PBD Pharmacophores. *J. Med. Chem.* **2003**, *46* (11), 2132−2151.
(30) Bose, D. S.; Thompson, A. S.; Smellie, M.; Berardini, M. D.; Hartley, J. A.; Jenkins, T. C.; Neidle, S.; Thurston, D. E. Effect of Linker Length on DNA-Binding Affinity, Cross-Linking Efficiency and Cytotoxicity of C8−Linked Pyrrolobenzodiazepine Dimers. *Chem. Commun.* **1992**, *20*, 1518−1520.
(31) Thurston, D. E.; Bose, D. S.; Thompson, A. S.; Howard, P. W.; Leoni, A.; Croker, S. J.; Jenkins, T. C.; Neidle, S.; Hartley, J. A.; Hurley, L. H. Synthesis of Sequence-Selective C8−Linked Pyrrolo[2,1-*c*]-[1,4]benzodiazepine DNA Interstrand Cross-Linking Agents. *J. Org. Chem.* **1996**, *61* (23), 8141−8147.
(32) Gregson, S. J.; Howard, P. W.; Corcoran, K. E.; Barcella, S.; Yasin, M. M.; Hurst, A. A.; Jenkins, T. C.; Kelland, L. R.; Thurston, D. E. Effect of C2-exo unsaturation on the cytotoxicity and DNA- binding reactivity of pyrrolo[2,1-*c*][1,4]benzodiazepines. *Bioorg. Med. Chem. Lett.* **2000**, *10* (16), 1845−1847.
(33) Gregson, S. J.; Howard, P. W.; Hartley, J. A.; Brooks, N. A.; Adams, L. J.; Jenkins, T. C.; Kelland, L. R.; Thurston, D. E. Design, Synthesis, and Evaluation of a Novel Pyrrolobenzodiazepine DNA-Interactive Agent with Highly Efficient Cross-Linking Ability and Potent Cytotoxicity. *J. Med. Chem.* **2001**, *44* (5), 737−748.
(34) Gregson, S. J.; Howard, P. W.; Jenkins, T. C.; Kelland, L. R.; Thurston, D. E. Synthesis of a novel C2/C2′-Exo unsaturated pyrrolobenzodiazepine cross-linking agent with remarkable DNA binding affinity and cytotoxicity. *Chem. Commun.* **1999**, *9*, 797−798.
(35) Gregson, S. J.; Howard, P. W.; Barcella, S.; Nakamya, A.; Jenkins, T. C.; Kelland, L. R.; Thurston, D. E. Effect of C2/C3-endo unsaturation on the cytotoxicity and DNA-binding reactivity of pyrrolo[2,1-*c*][1,4]benzodiazepines. *Bioorg. Med. Chem. Lett.* **2000**, *10* (16), 1849−1851.
(36) Smellie, M.; Bose, D. S.; Thompson, A. S.; Jenkins, T. C.; Hartley, J. A.; Thurston, D. E. Sequence-Selective Recognition of Duplex DNA Through Covalent Interstrand Cross-Linking: Kinetic and Molecular Modeling Studies With Pyrrolobenzodiazepine Dimers. *Biochemistry* **2003**, *42* (27), 8232−8239.
(37) Gregson, S. J.; Howard, P. W.; Gullick, D. R.; Hamaguchi, A.; Corcoran, K. E.; Brooks, N. A.; Hartley, J. A.; Jenkins, T. C.; Patel, S.; Guille, M. J.; Thurston, D. E. Linker Length Modulates DNA Cross-Linking Reactivity and Cytotoxic Potency of C8/C8′ Ether-Linked C2-Exo-Unsaturated Pyrrolo[2,1-*c*][1,4]benzodiazepine (PBD) Dimers. *J. Med. Chem.* **2004**, *47* (5), 1161−1174.
(38) Gregson, S. J.; Howard, P. W.; Corcoran, K. E.; Jenkins, T. C.; Kelland, L. R.; Thurston, D. E. Synthesis of the First Example of a C2-C3/C2′-C3′-Endo Unsaturated Pyrrolo[2,1-*c*][1,4]benzodiazepine Dimer. *Bioorg. Med. Chem. Lett.* **2001**, *11* (21), 2859−2862.
(39) Jones, G. B.; Davey, C. L.; Jenkins, T. C.; Kamal, A.; Kneale, G. G.; Neidle, S.; Webster, G. D.; Thurston, D. E. The Non-Covalent Interaction of Pyrrolo[2,1-*c*][1,4]benzodiazepine-5,11-diones with DNA. *Anti-Cancer Drug Des.* **1990**, *5* (3), 249−264.
(40) Martin, C.; Ellis, T.; McGurk, C. J.; Jenkins, T. C.; Hartley, J. A.; Waring, M. J.; Thurston, D. E. Sequence-Selective Interaction of the Minor-Groove Interstrand Cross-Linking Agent SJG-136 with Naked and Cellular DNA: Footprinting and Enzyme Inhibition Studies. *Biochemistry* **2005**, *44* (11), 4135−4147.
(41) Cooper, N.; Burger, A. M.; Matthews, C. S.; Howard, P. W.; Thurston, D. E. Structure-Activity-Relationship (SAR) Study of Novel C2/C3−Unsaturated C2-Aryl-Substituted Pyrrolobenzodiazepine Monomer Antitumour Agents. *Eur. J. Cancer* **2002**, *38*, 404.
(42) Cooper, N.; Hagan, D. R.; Tiberghien, A.; Ademefun, T.; Matthews, C. S.; Howard, P. W.; Thurston, D. E. Synthesis of Novel C2-Aryl Pyrrolobenzodiazepines (PBDs) as Potential Antitumour Agents. *Chem. Commun.* **2002**, (16), 1764−1765.
(43) Frisch, M. J.; Trucks, G. W.; Schlegel, H. B.; Scuseria, G. E.; Robb, M. A.; Cheeseman, J. R.; Zakrzewski, V. G.; Montgomery, J. A.; Stratmann, R. E.; Burant, J. C.; Dapprich, S.; Millam, J. M.; Daniels, A. D.; Kudin, K. N.; Strain, M. C.; Farkas, O.; Tomasi, J.; Barone, V.; Cossi, M.; Cammi, R.; Mennucci, B.; Pomelli, C.; Adamo, C.; Clifford, S.; Ochterski, J.; Petersson, G. A.; Ayala, P. Y.; Cui, Q.; Morokuma, K.; Malick, D. K.; Rabuck, A. D.; Raghavachari, K.; Foresman, J. B.; Cioslowski, J.; Ortiz, J. V.; Stefanov, B. B.; Liu, G.; Liashenko, A.; Piskorz, P.; Komaromi, I.; Gomperts, R.; Martin, R. L.; Fox, D. J.; Keith, T.; Al-Laham, M. A.; Peng, C. Y.; Nanayakkara, A.; Gonzalez, C.; Challacombe, M.; Gill, P. M. W.; Johnson, B. G.; Chen, W.; Wong, M. W.; Andres, J. L.; Head-Gordon, M.; Replogle, E. S.; Pople, J. A., Gaussian, Inc., Pittsburgh, PA, 1998.
(44) Case, D. A.; Pearlman, D. A.; Caldwell, J. W.; Cheatham, T. E., III; Wang, J.; Ross, W. S.; Simmerling, C. L.; Darden, T. A.; Merz, K. M.; Stanton, R. V.; Cheng, A. L.; Vincent, J. J.; Crowley, M.; Tsui, V.; Gohlke, H.; Radmer, R. J.; Duan, Y.; Pitera, J.; Massova, I.; Seibel, G. L.; Singh, U. C.; Weiner, P. K.; Kollman, P. A. AMBER 7. University of California, San Francisco, 2002.
(45) Bayly, C. I.; Cieplak, P.; Cornell, W. D.; Kollman, P. A. A Well-Behaved Electrostatic Potential Based Method Using Charge Restraints For Deriving Atomic Charges − the Resp Model. *J. Phys. Chem.* **1993**, *97* (40), 10269−10280.
(46) Wang, J. M.; Cieplak, P.; Kollman, P. A. How Well Does a Restrained Electrostatic Potential (RESP) Model Perform in Calculating Conformational Energies of Organic and Biological Molecules? *J. Comput. Chem.* **2000**, *21* (12), 1049−1074.
(47) Tsui, V.; Case, D. A. Molecular Dynamics Simulations of Nucleic Acids with a Generalized Born Solvation Model. *J. Am. Chem. Soc.* **2000**, *122* (11), 2489−2498.
(48) Srinivasan, J.; Cheatham, T. E.; Cieplak, P.; Kollman, P. A.; Case, D. A. Continuum Solvent Studies of the Stability of DNA, RNA, and Phosphoramidate-DNA Helices. *J. Am. Chem. Soc.* **1998**, *120* (37), 9401−9409.
(49) McConnaughie, A. W.; Jenkins, T. C. Novel Acridine-Triazenes as Prototype Combilexins − Synthesis, DNA-Binding, and Biological-Activity. *J. Med. Chem.* **1995**, *38* (18), 3488−3501.
(50) Manzini, G.; Barcellona, M. L.; Avitabile, M.; Quadrifoglio, F. Interaction of Diamidino-2-Phenylindole (DAPI) with Natural and Synthetic Nucleic Acids. *Nucleic Acids Res.* **1983**, *11* (24), 8861−8876.
(51) Trauger, J. W.; Dervan, P. B. Footprinting Methods for Analysis of Pyrrole-Imidazole Polyamide/DNA Complexes. In *Drug-Nucleic Acid Interactions*; Academic Press Inc: San Diego, 2001; Vol. 340, pp 450−466.
(52) Bose, D. S.; Thompson, A. S.; Ching, J. S.; Hartley, J. A.; Berardini, M. D.; Jenkins, T. C.; Neidle, S.; Hurley, L. H.; Thurston, D. E. Rational Design of a Highly Efficient Irreversible DNA Interstrand Cross-Linking Agent Based on the Pyrrolobenzodiazepine Ring-System. *J. Am. Chem. Soc.* **1992**, *114* (12), 4939−4941.

JM051199Z